**GPH-International Journal of Mathematics**
(Online ISSN 3050-9645)
Volume 08 | Issue 02 | 2025
Published by **Global Publication House**
**DOI**: https://doi.org/10.5281/zenodo.21395541
Available online at www.gphjournal.org
Journal homepage: https://gphjournal.org/index.php/m/index

# Impact of Screening and Contact Tracing on a Deterministic Compartmental Model for Chlamydia Transmission Dynamics

**Jibrin Danjuma Yahaya[1], Agbata Benedict Celestine[1], Ugo Donald Chukwuma[2], Okofu Mary Bassey[3], Acheneje Godwin Onuche[4], Jacob Funsho Omonile[5], Emmanuel Ogala[6]**

*[1]Department of Mathematics and Statistics, Confluence University of Science and Technology, Osara, Kogi State, Nigeria*
*[2]Department of Mathematics, Enugu State University of Science and Technology, Agbani, Nigeria.*
*[3]Department of Mathematics University of Nigeria, Nsukka, Nigeria.*
*[4]Department of Mathematics Prince Abubakar Audu University, Anyigba, Nigeria.*
*[5]Department of Physics, Confluence University of Science and Technology, Osara, Kogi State, Nigeria.*
*[6]Department of Computer Science, College of Physical Sciences, Joseph Sarwuan Tarka University, Makurdi.*
Corresponding Author: Okofu Mary Bassey E-mail: *mary.okofu@unn.edu.ng*

## Abstract:

*Chlamydia trachomatis* remains the most prevalent bacterial sexually transmitted infection worldwide, with over 128 million new cases reported annually. Despite the availability of effective treatment, its largely asymptomatic nature and high reinfection rates continue to sustain transmission, posing a major public health concern. In this study, a seven-compartment deterministic model is developed to investigate the transmission dynamics of *Chlamydia trachomatis*. The model incorporates key epidemiological features, including screening detection with reduced infectiousness, partial waning immunity, and realistic treatment pathways. Using the next-generation matrix method, the basic reproduction number is derived, confirming the potential for endemic persistence under baseline parameter values. Stability analysis shows that the disease-free equilibrium is locally asymptotically stable when the reproduction number is less than one and unstable otherwise. Furthermore, the endemic equilibrium is proven to be globally asymptotically stable under certain conditions using Lyapunov methods, with the possibility of backward bifurcation indicating that reducing the reproduction number below unity may not be sufficient for disease elimination. Normalized sensitivity analysis identifies condom efficacy as the most influential parameter in reducing transmission, followed by treatment success rate, duration of immunity, and symptomatic care-seeking behavior. In contrast, transmission probability and infectiousness during screening exert strong positive effects on disease spread, while disease-induced mortality parameters have minimal impact on overall dynamics. The model highlights the critical role of the large asymptomatic population in sustaining transmission and demonstrates that rapid

waning of immunity, approximately 180 days, contributes significantly to high reinfection rates. The findings emphasize that effective control of *Chlamydia trachomatis* requires integrated intervention strategies. These include sustained condom promotion, expansion of targeted screening programs, minimization of diagnostic delays, and efficient partner notification systems. Additionally, repeat testing protocols are essential to address reinfection driven by short-lived immunity.

## Keywords:

*Chlamydia trachomatis, Transmission dynamics, Basic reproduction number, Sensitivity analysis, Simulations.*

## Introduction

Chlamydia is one of the most prevalent sexually transmitted infections (STIs) globally and continues to pose a major challenge to public health systems. It is caused by the bacterium *Chlamydia trachomatis* and primarily affects the urogenital tract, although infections can also occur in the rectum, throat, and eyes. The infection is particularly concerning because it is frequently asymptomatic, allowing it to spread silently within populations and remain undetected for long periods [1][2]. This asymptomatic nature contributes significantly to its high transmission rate and persistent global burden. Globally, chlamydia remains highly widespread, with millions of new infections reported annually. According to recent estimates, approximately 128.5 million new cases occurred worldwide among individuals aged 15–49 years in 2020, making it one of the most common bacterial STIs [1][3]. In addition, surveillance data from developed regions such as Europe indicate a steady increase in reported cases, with over 230,000 confirmed infections recorded in 2023 alone [4]. Similarly, in the United States, more than 1.6 million cases were reported in 2023, further confirming its status as the most frequently reported STI [5]. These statistics highlight the continued global spread of chlamydia, particularly among young people and high-risk populations [3][5].

Transmission of chlamydia occurs mainly through unprotected vaginal, anal, or oral sexual contact with an infected individual. It can also be transmitted from an infected mother to her newborn during childbirth, potentially causing serious neonatal complications such as conjunctivitis and pneumonia [1][6]. Although many individuals do not exhibit symptoms, untreated infections can lead to severe health outcomes, including pelvic inflammatory disease, infertility, ectopic pregnancy in women, and epididymitis in men [1][7]. Furthermore, chlamydia infection has been associated with an increased risk of acquiring and transmitting other infections, including HIV [1][8]. These complications underscore the importance of early detection and treatment. The burden of chlamydia is influenced by several social and healthcare-related factors, including limited access to screening services, stigma associated with STIs, and variations in public health infrastructure. In many low- and middle-income countries, underdiagnosis and underreporting remain significant challenges due to inadequate diagnostic facilities and lack of awareness [3][9]. Even in high-income regions, differences in testing strategies and surveillance systems contribute to variations in reported prevalence rates [4][10]. These disparities make it difficult to accurately assess the true global burden of the disease and emphasize the need for improved surveillance and equitable access to healthcare services.

Efforts to control and prevent chlamydia focus on a combination of strategies, including routine screening, early diagnosis, effective antibiotic treatment, and public health

education. The use of nucleic acid amplification tests (NAATs) has significantly improved diagnostic accuracy, enabling timely identification of infections [1][11]. Additionally, consistent condom use and partner notification are key preventive measures that help reduce transmission [1][12]. Mathematical modeling and epidemiological studies have also become essential tools in understanding transmission patterns and evaluating the impact of intervention strategies, thereby supporting informed decision-making in public health policy [13]. Strengthening these approaches is critical to reducing the global burden of chlamydia and improving reproductive health outcomes.

Recent studies have increasingly applied mathematical modeling techniques to better understand the transmission dynamics and control of chlamydia. These models have incorporated advanced analytical methods, including fractional calculus, compartmental modeling, and numerical simulations, to provide insights into disease behavior and intervention strategies. Alqahtani et al. [14] developed a fractional-order mathematical model to describe the spread of chlamydia using Caputo derivatives. The study established key mathematical properties such as positivity, boundedness, and existence of solutions, confirming the model's biological feasibility. The authors demonstrated that the disease-free equilibrium was locally asymptotically stable when the basic reproduction number was less than one, while a unique endemic equilibrium existed when it exceeded one. Sensitivity analysis further identified the most influential parameters affecting disease transmission, highlighting the importance of targeted control strategies. Nisar et al [15] proposed a fractional-order model incorporating vaccination dynamics and chaotic behavior analysis. Their work utilized a generalized fractal-fractional operator to explore the qualitative behavior of the system. The study showed that vaccination plays a crucial role in reducing infection levels and stabilizing the system. The results emphasized that incorporating vaccination into modeling frameworks significantly improves predictions of disease control outcomes.

Farrell et al [16] examined the impact of screening strategies on the health burden of chlamydia using a compartmental modeling approach. Their model introduced the concept of "person-days of infection" to evaluate disease burden more effectively. The findings indicated that increased screening frequency substantially reduced infection duration and overall disease burden. The study highlighted screening as a critical intervention for controlling asymptomatic infections, which are common in chlamydia cases. Nyerere and Liana [17] investigated the effects of combined control strategies, including treatment, vaccination, and public health education, on chlamydia transmission dynamics. Using a deterministic compartmental model, the authors derived the basic reproduction number and conducted sensitivity analysis. Their results showed that a combination of interventions was more effective than single strategies, with education and treatment significantly reducing disease prevalence. Odeh et al [18] developed a compartmental model focusing on treatment strategies for controlling chlamydia transmission. The population was divided into multiple classes, including susceptible, exposed, infected, treated, and recovered individuals. The study demonstrated that effective treatment and timely intervention could significantly reduce infection levels. Numerical simulations supported the conclusion that strengthening treatment programs is essential for disease control.

The aim of this research is to formulate and analyse a deterministic mathematical model of *Chlamydia trachomatis* transmission dynamics that incorporates screening detection pathways, differential infectiousness during screening and treatment, partial immunity, and long-term sequelae-induced mortality, in order to evaluate the effectiveness of existing and improved control strategies. To achieve this aim, the objectives are to: (i) develop a compartmental mathematical model for *Chlamydia trachomatis* transmission

and compute the basic reproduction number using the next-generation matrix approach; (ii) establish the existence and examine the local and global stability of both disease-free and endemic equilibrium states; (iii) conduct sensitivity analysis in order to identify key parameters that significantly influence transmission dynamics and disease prevalence; (iv) perform numerical simulations assessing the impact of screening coverage, treatment delays, partner notification effectiveness, and post-testing behavioural risk reduction on long-term infection prevalence and complication incidence; and (v) provide evidence-based recommendations for improving and optimizing chlamydia control programmes across diverse epidemiological settings.

The novelty of this study lies in the development of a detailed and realistic compartmental framework that captures key epidemiological and behavioural processes involved in the transmission dynamics of *Chlamydia trachomatis*. Unlike many existing models, this study explicitly incorporates a screening compartment that reflects routine and opportunistic detection pathways, thereby distinguishing between individuals who are identified early through screening and those who remain undetected. This inclusion allows for a more accurate representation of real-world public health interventions and their impact on disease dynamics. A further innovative aspect of the model is the differentiation between asymptomatic and symptomatic infectious individuals, with distinct transition pathways and detection mechanisms. The model captures the progression from exposure to asymptomatic infection, followed by possible symptom development or detection through partner notification and re-screening. This dual pathway structure provides a more comprehensive understanding of hidden transmission, which is a major challenge in chlamydia control due to the high proportion of asymptomatic cases. Additionally, the model uniquely integrates multiple entry points into treatment, including screening-positive individuals, detected asymptomatic cases, and symptomatic individuals seeking care. By doing so, it reflects the diverse routes through which infected individuals access treatment services. The incorporation of treatment outcomes leading to recovery, alongside the inclusion of waning immunity that returns individuals to the susceptible class, further enhances the biological realism of the model. The study advances existing modeling approaches by combining screening dynamics, differential infectious stages, varied detection pathways, and temporary immunity within a single unified framework. This integrated structure provides deeper insights into the role of early detection, treatment strategies, and reinfection in sustaining transmission, thereby offering a more robust tool for evaluating and optimizing chlamydia control interventions.

## Model formulation

The recruitment rate of sexually active humans into the susceptible population is given as $\lambda$. Susceptible individuals ($S$) acquire Chlamydia trachomatis infection through effective contact with infectious individuals at the force of infection $\Lambda$ and move to the exposed (latent) compartment ($E$). From the exposed compartment ($E$), individuals progress in two possible directions: a fraction is identified through routine or opportunistic screening programmes and moves to the screening class ($S_R$) at rate $\alpha_E$, while the remaining fraction progresses to the asymptomatic infectious compartment ($I_A$) at rate $\alpha_{IA}$. Individuals in the screening class ($S_R$) who test negative return to the susceptible class ($S$) at rate $\varepsilon$. Those who test positive are initiated on treatment at rate $\omega_{SR}$ and move to the treatment compartment ($T$).

Asymptomatic infectious individuals ( $I_A$ ) may develop symptoms and progress to the symptomatic infectious compartment ( $I_S$ ) at rate $\tau$ , or be detected (e.g., via partner notification or re-screening) and enter treatment at rate $\omega_A$ , moving to the treatment compartment ( $T$ ). Symptomatic infectious individuals ( $I_S$ ) seek care because of symptoms and are placed on treatment at rate $\omega_S$ , thereby entering the treatment compartment ( $T$ ). All individuals receiving treatment in compartment $T$ (from $S_R$ , $I_A$ , or $I_S$ ) clear the infection and recover at rate $\psi$ , moving to the recovered compartment ( $R$ ). Recovered individuals ( $R$ ) gradually lose protective immunity and return to the susceptible class ( $S$ ) at rate $\theta$ .

Natural mortality occurs in every compartment at constant rate $\mu$ . Disease-induced mortality arising from long-term complications of chlamydia occurs in the screening class at rate $\delta_{SR}$ , in the asymptomatic infectious class at rate $\delta_A$ , in the symptomatic infectious class at rate $\delta_S$ , and in the treatment class at rate $\delta_T$ .

The formulation of the *Chlamydia trachomatis* transmission model is based on the following assumptions:

(i) The sexually active human population is assumed to mix homogeneously, meaning that each individual has an equal probability of coming into contact with any other individual. The force of infection follows a standard incidence form and depends on the proportion of infectious individuals in the population, including asymptomatic, symptomatic, and individuals undergoing treatment who may still transmit the infection during the early stages of therapy [19,20, 21].

(ii) The natural death rate is assumed to be constant across all compartments. However, disease-induced mortality occurs only among infected individuals, including those in the asymptomatic, symptomatic, and treatment classes, due to long-term complications associated with untreated or poorly managed chlamydia, such as pelvic inflammatory disease, ectopic pregnancy, infertility, and increased susceptibility to HIV infection [22,23,24].

(iii) Individuals in the exposed (latent) class progress through two possible pathways. A proportion is detected through routine or opportunistic screening programs and moves into the screening class, while the remaining proportion progresses to the asymptomatic infectious class. This assumption reflects the largely asymptomatic nature of chlamydia infections, particularly among women and men, where a significant percentage of cases remain undiagnosed without active screening [25,26,27].

(iv) Recovery from infection does not confer permanent immunity. Individuals who recover from chlamydia gradually lose any temporary protection and return to the susceptible class, making them vulnerable to reinfection. This assumption aligns with epidemiological evidence indicating frequent reinfections and only partial or short-lived natural immunity [28,29].

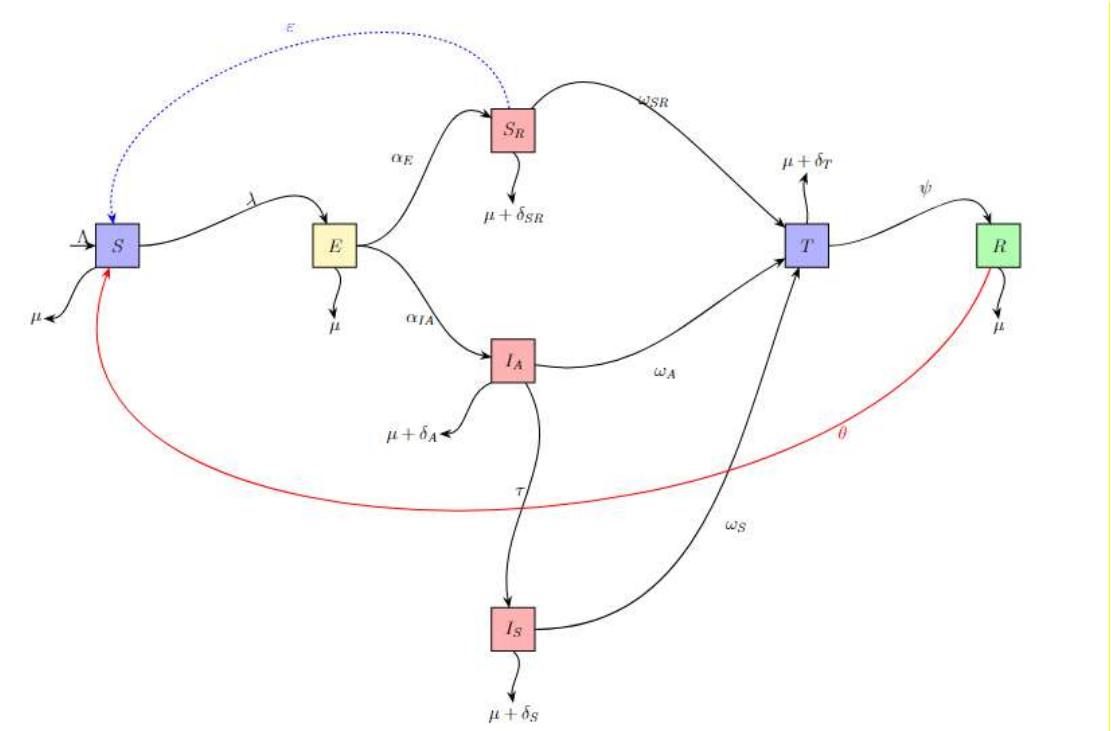


**Figure 1:** Schematic Diagram of the chlamydia model

The system of ordinary differential equations governing the model is:

$$\frac{dS}{dt} = \Lambda + \varepsilon S_R + \theta R - (\lambda + \mu) S$$

$$\frac{dE}{dt} = \lambda S - (\alpha_E + \alpha_{IA} + \mu) E$$

$$\frac{dS_R}{dt} = \alpha_E E - (\omega_{SR} + \varepsilon + \mu + \delta_{SR}) S_R$$

$$\frac{dI_A}{dt} = \alpha_{IA} E - (\tau + \omega_A + \mu + \delta_A) I_A$$

$$\frac{dI_S}{dt} = \tau I_A - (\omega_S + \mu + \delta_S) I_S$$

$$\frac{dT}{dt} = \omega_{SR} S_R + \omega_A I_A + \omega_S I_S - (\psi + \mu + \delta_T) T$$

$$\frac{dR}{dt} = \psi T - (\theta + \mu) R$$

The total population is

$$N = S + E + S_R + I_A + I_S + T + R$$

The force of infection is given by standard incidence:

$$\lambda = \beta(1-\gamma)\frac{\phi S_R + I_A + I_S + T}{N}$$

Let $k_1 = (\alpha_E + \alpha_{IA} + \mu)$, $k_2 = (\omega_{SR} + \varepsilon + \mu + \delta_{SR})$, $k_3 = (\tau + \omega_A + \mu + \delta_A)$,

$$k_4 = (\omega_S + \mu + \delta_S), k_5 = (\psi + \mu + \delta_T), \; k_6 = (\theta + \mu)$$

**Table 1: Model variables and their descriptions**

| Variable | Description |
|---|---|
| $S$ | Susceptible individuals |
| $E$ | Exposed (latent) individuals |
| $S_R$ | Individuals detected by screening (awaiting treatment) |
| $I_A$ | Asymptomatically infected individuals |
| $I_S$ | Symptomatically infected individuals |
| $T$ | Individuals under treatment |
| $R$ | Recovered individuals (temporary immunity) |

**Model parameters and their descriptions**

| Parameter | Description |
|---|---|
| $\lambda$ | Recruitment rate into susceptible class |
| $\beta$ | Transmission coefficient |
| $\Lambda$ | Force of infection |
| $\mu$ | Natural death rate |
| $\alpha_E$ | Progression rate from $E$ to $S_R$ (screen-detected) |
| $\alpha_{IA}$ | Progression rate from $E$ to $I_A$ |
| $\varepsilon$ | Rate of return to $S$ after negative screening |
| $\beta$ | contact rate of susceptible humans and infectious classes |
| $\gamma$ | Rate of compliance to safe sex practice |
| $\phi$ | modification parameter accounting for reduced disease transmission in the test screening class |
| $\omega_{SR}$ | Treatment rate of screen-detected individuals |
| $\omega_A$ | Treatment/detection rate of asymptomatic carriers |

| | |
|---|---|
| $\omega_S$ | Treatment rate of symptomatic individuals |
| $\tau$ | Rate of symptom development |
| $\psi$ | Recovery rate from treatment |
| $\theta$ | Rate of loss of immunity |
| $\delta_{SR}, \delta_A, \delta_S, \delta_T$ | Disease-induced death rates |
| $\phi$ | Relative infectiousness of symptomatic individuals |
| $\xi$ | Relative infectiousness during treatment . |

## Model Analysis

### Positivity and Boundedness of Solutions

To ensure that the model is mathematically well-posed and epidemiologically meaningful, we prove that all state variables remain non-negative and bounded for all time $t \geq 0$ whenever the initial conditions are non-negative.

### Theorem 1 (Positivity of Solutions)

Let the initial conditions be

$S(0) > 0, E(0) > 0, S\_R(0) > 0, I\_A(0) > 0, I\_S(0) > 0, T(0) > 0, R(0) > 0.$

Then the solutions $(S(t), E(t), S_R(t), I_A(t), I_S(t), T(t), R(t))$ of the Chlamydia trachomatis model are non-negative for all $t > 0$.

### Proof

We use the standard contradiction argument. Define

$$t_1 = supt > 0 : S(\tau) > 0, E(\tau) = 0, S_R(\tau) = 0, I_A(\tau) = 0, I_S(\tau) = 0, T(\tau) = 0,$$

$$R(\tau) = 0, \ \tau[0,t].$$

Clearly $t_1 > 0$ since the initial data satisfy the conditions.

$$\frac{dS}{dt} = \lambda + \varepsilon S_R + \theta R - \Lambda S - \mu S \geq -(\Lambda(t) + \mu)S$$

Integrating from 0 to t gives

$$S(t) \geq S(0)\exp\left(-\int_0^t (\Lambda(s) + \mu)ds\right) > 0 \quad \forall t \geq 0,$$

because the exponential is always positive. Thus $S(t) > 0$ for all $t \geq 0$.

$$\frac{dE}{dt} = \Lambda S - (\alpha_E + \alpha_{IA} + \mu)E \geq -(\alpha_E + \alpha_{IA} + \mu)E.$$

Hence

$$E(t) \geq E(0)\exp\left(-(\alpha_E + \alpha_{IA} + \mu)t\right) \geq 0.$$

For $S_R, I_A, I_S, T$, and $R$, the differential equations have the general form

$$\frac{dX}{dt} = (\text{sum of non-negative inflow terms}) - (\text{progression/treatment rate})X - (\mu + \delta_X)X,$$

where $\delta_X = 0(\delta_{SR}, \delta_A, \delta_S, \delta_T) and \delta_R = 0$.

When $X(t)?0^?$, the inflow terms are non-negative, so

$$\frac{dX}{dt} \geq -k_X X \quad \text{with} \quad k_X = \text{progression/treatment rate} + \mu + \delta_X > 0.$$

This implies

$$X(t) \geq X(0)\exp\left(-\int_0^t k_X(s)ds\right) \geq 0.$$

Suppose, for contradiction, that there exists a first time $\tau \leq t_1$ where one of these variables (say X(τ) = 0) while it was positive before. Then at τ, the non-negative inflow would force dX/dt ≥ 0, contradicting X becoming negative or crossing zero downwards. Hence all compartments remain non-negative up to $t_1$. Since $t_1$ was chosen maximally, $t_1 = +\infty$.

Therefore, all state variables are non-negative for all t > 0, and S(t) is strictly positive.

**Invariant Region and Boundedness**

**Theorem 2**

Given that

$$\Omega = \left\{(S, E, S_R, I_A, I_S, T, R) \in \mathbb{R}^7_{\geq 0} : N(t) = S + E + S_R + I_A + I_S + T + R \leq \frac{\lambda}{\mu}\right\}$$

is positively invariant and globally attracting for the model trajectories with non-negative initial conditions.

**Proof**

Differentiating the total population $N(t)$:

$$\frac{dN}{dt} = \lambda + \varepsilon S_R + \theta R - \Lambda S - \mu(S + E + R)$$

$$-(\mu + \delta_{SR})S_R - (\mu + \delta_A)I_A - (\mu + \delta_S)I_S - (\mu + \delta_T)T$$

$$= \lambda - \mu N - \delta_{SR}S_R - \delta_A I_A - \delta_S I_S - \delta_T T$$

$$\leq \lambda - \mu N.$$

Thus,

$$\frac{dN}{dt} + \mu N \leq \lambda.$$

Multiplying by the integrating factor $e^{\mu t}$ and integrating yields

$$N(t) \leq N(0)e^{-\mu t} + \frac{\Lambda}{\mu}(1 - e^{-\mu t}).$$

Hence,

$$N(t) \leq \max\left\{N(0), \frac{\Lambda}{\mu}\right\}.$$

As $t \to \infty, N(t) \leq \frac{\Lambda}{\mu}$, and the upper bound λ/μ is attained only in the disease-free case.

Moreover, if $N(t) = \frac{\Lambda}{\mu}$ and $N(t) > \frac{\Lambda}{\mu}$ is attempted, then dN/dt $<$ 0, so trajectories cannot leave Ω. On the boundary faces where any compartment is zero, the corresponding inflows are non-negative, preventing solutions from exiting $\mathbb{R}_+^7$. Therefore, Ω is positively invariant and attracts all solutions in $\mathbb{R}_+^7$.

**Disease-Free Equilibrium (DFE)**

The disease-free equilibrium is obtained by setting all infected-related compartments to zero:

$$E = S_R = I_A = I_S = T = R = 0.$$

The only non-trivial equation remaining is

$$\frac{dS}{dt} = \lambda - \mu S = 0 \quad \Rightarrow \quad S^0 = \frac{\lambda}{\mu}.$$

The total population at DFE is $N^0 = S^0 = \frac{\lambda}{\mu}$

Thus, the unique disease-free equilibrium of the model is

$$\mathrm{E}_0 = \left( \frac{\lambda}{\mu}, 0, 0, 0, 0, 0, 0 \right).$$

**Basic reproduction number of the chlamydia model**

The basic reproduction number of the chlamydia model is the threshold parameter that determines the number of secondary cases of chlamydia infection that will occur due to the introduction of an infectious chlamydia individual into a wholly susceptible population.

The basic reproduction number is obtained using the next generation operator matrix as postulated by [30]. Which is given by $\rho(FV^{-}1)$.

Where $F$ is the matrix of new infection and $V$ is the matrix of the transient term.

$$F = \begin{bmatrix} 0 & \beta(1-\gamma)\phi & \beta(1-\gamma) & \beta(1-\gamma) & \beta(1-\gamma) \\ 0 & 0 & 0 & 0 & 0 \\ 0 & 0 & 0 & 0 & 0 \\ 0 & 0 & 0 & 0 & 0 \\ 0 & 0 & 0 & 0 & 0 \end{bmatrix},$$

$$V = \begin{bmatrix} k_1 & 0 & 0 & 0 & 0 \\ -\alpha_E & k_2 & 0 & 0 & 0 \\ -\alpha_{IA} & 0 & k_3 & 0 & 0 \\ 0 & 0 & -\tau & k_4 & 0 \\ 0 & -\omega_{SR} & -\omega_A & \omega_S & k_5 \end{bmatrix}$$

$$FV^{-1} = \begin{bmatrix} -\frac{\left(\left((k_5+\omega_A)k_4 - \tau(-k_5+\omega_S)\right)\alpha_{IA}k_2 + \alpha_E k_3 k_4(\phi k_5 + \omega_{SR})\right)\beta(-1+\gamma)}{k_1 k_2 k_3 k_4 k_5} & -\frac{\beta(-1+\gamma)(\phi k_5 + \omega_{SR})}{k_2 k_5} & -\frac{\beta\left((k_5+\omega_A)k_4 + \tau(k_5-\omega_S)\right)(-1+\gamma)}{k_3 k_4 k_5} & -\frac{\beta(-1+\gamma)(k_5-\omega_S)}{k_4 k_5} & \frac{\beta(1-\gamma)}{k_5} \\ 0 & 0 & 0 & 0 & 0 \\ 0 & 0 & 0 & 0 & 0 \\ 0 & 0 & 0 & 0 & 0 \\ 0 & 0 & 0 & 0 & 0 \end{bmatrix}$$

The dominant eigenvalue of $FV^{-1}$ is given below which is the basic reproduction number of the chlamydia model

$$R_0 = \frac{\beta(1-\gamma)\left(\left((k_5+\omega_A)k_4 + \tau(k_5-\omega_S)\right)\alpha_{IA}k_2 + \alpha_E k_3 k_4(\phi k_5 + \omega_{SR})\right)}{k_1 k_2 k_3 k_4 k_5}$$

**Local Asymptotic Stability of the disease free equilibrium point of the chlamydia model**

**Theorem 3**

The chlamydia model $R_0$ is locally asymptotically stable if $R_0 < 1$ and unstable if $R_0 > 1$.

**Proof**

To prove the local asymptotic stability of the disease free equilibrium of the chlamydia model, we take the jacobian matrix of the system (1).

The jacobian matrix of the system is given as $J(\varepsilon_0)$

$$J(\varepsilon_0) = \begin{bmatrix} -\mu & 0 & \grave{o}-\beta(1-\gamma)\phi & -\beta(1-\gamma) & -\beta(1-\gamma) & \beta(1-\gamma) & \theta \\ 0 & -k_1 & \beta(1-\gamma)\phi & \beta(1-\gamma) & \beta(1-\gamma) & \beta(1-\gamma) & 0 \\ 0 & \alpha_E & -k_2 & 0 & 0 & 0 & 0 \\ 0 & \alpha_{IA} & 0 & -k_3 & 0 & 0 & 0 \\ 0 & 0 & 0 & \tau & -k_4 & 0 & 0 \\ 0 & 0 & \omega_{SR} & \omega_A & \omega_S & -k_5 & 0 \\ 0 & 0 & 0 & 0 & 0 & \psi & k_6 \end{bmatrix}$$

The first and seventh columns of the jacobian matrix $J(\varepsilon_0)$ consists of only $-\mu$ and $k_6$ which consists of the first two eigenvalues of the system, the remaining eigenvalues of the system are obtained from the reduced system which yields the new matrix $J_1(\varepsilon_0)$ given below as:

$$J_1(\varepsilon_0) = \begin{bmatrix} -k_1 & \beta(1-\gamma)\phi & \beta(1-\gamma) & \beta(1-\gamma) & \beta(1-\gamma) \\ \alpha_E & -k_2 & 0 & 0 & 0 \\ \alpha_{IA} & 0 & -k_3 & 0 & 0 \\ 0 & 0 & \tau & -k_4 & 0 \\ 0 & \omega_{SR} & \omega_A & \omega_S & -k_5 \end{bmatrix}$$

The characteristics polynomial of the reduced $J_1(\varepsilon_0)$ is given as

$$\lambda^5 - (-k_5 - k_4 - k_3 - k_2 - k_1)$$

$$+\lambda^4 - (-\beta\gamma\phi\alpha_E - \beta\gamma\alpha_{IA} + \alpha_E\beta\phi + \alpha_{IA}\beta - k_2k_1 - k_3k_1 - k_4k_1 - k_5k_1 - k_3k_2 - k_4k_2 - k_5k_2 - k_4k_3 - k_5k_3 - k_5k_4$$

$$\lambda^3 - (-\beta\gamma k_3\phi\alpha_E - \beta\gamma k_4\phi\alpha_E - \beta\gamma k_5\phi\alpha_E - \beta\gamma k_2\alpha_{IA} - \beta\gamma k_4\alpha_{IA} - \beta\gamma k_5\alpha_{IA} - \beta\gamma\tau\alpha_{IA} - \beta\gamma\alpha_E\omega_{SR}$$

$$-\beta\gamma\alpha_{IA}\omega_A + \beta k_3\phi\alpha_E + \beta k_4\phi\alpha_E + \beta k_5\phi\alpha_E + \beta k_2\alpha_{IA} + \beta k_4\alpha_{IA} + \beta k_5\alpha_{IA} + \tau\alpha_{IA}\beta$$

$$+\omega_{SR}\alpha_E\beta + \omega_A\alpha_{IA}\beta - k_1k_2k_3 - k_1k_2k_4 - k_1k_2k_5 - k_1k_3k_4 - k_1k_3k_5 - k_1k_4k_5 - k_2k_3k_4 - k_2k_3k_5 - k_2k_4k_5 - k_3k_4k$$

$$\lambda^2 - (-\beta\gamma k_3k_4\phi\alpha_E - \beta\gamma k_3k_5\phi\alpha_E - \beta\gamma k_4k_5\phi\alpha_E - \beta\gamma k_2k_4\alpha_{IA} - \beta\gamma k_2k_5\alpha_{IA}$$

$$-\beta\gamma k_2\tau\alpha_{IA} - \beta\gamma k_2\alpha_{IA}\omega_A - \beta\gamma k_3\alpha_E\omega_{SR} - \beta\gamma k_4k_5\alpha_{IA} - \beta\gamma k_4\alpha_E\omega_{SR} - \beta\gamma k_4\alpha_{IA}\omega_A$$

$$-\beta\gamma k_5\tau\alpha_{IA}-\beta\gamma\tau\alpha_{IA}\omega_S+\beta k_3k_4\phi\alpha_E+\beta k_3k_5\phi\alpha_E+\beta k_4k_5\phi\alpha_E+\beta k_2k_4\alpha_{IA}+\beta k_2k_5\alpha_{IA}$$
$$+\beta k_2\tau\alpha_{IA}+\beta k_2\alpha_{IA}\omega_A+\beta k_3\alpha_E\omega_{SR}$$
$$+\beta k_4k_5\alpha_{IA}+\beta k_4\alpha_E\omega_{SR}+\beta k_4\alpha_{IA}\omega_A+\beta k_5\tau\alpha_{IA}+\beta\tau\alpha_{IA}\omega_S-k_1k_2k_3k_4$$
$$-k_1k_2k_3k_5-k_1k_2k_4k_5-k_1k_3k_4k_5-k_2k_3k_4k_5\big)$$
$$\lambda+\beta\gamma k_3k_4k_5\phi\alpha_E+\beta\gamma k_2k_4k_5\alpha_{IA}+\beta\gamma k_2k_4\alpha_{IA}\omega_A+\beta\gamma k_2k_5\tau\alpha_{IA}+\beta\gamma k_2\tau\alpha_{IA}\omega_S+\beta\gamma k_3k_4\alpha_E\omega_{SR}$$
$$-\beta k_3k_4k_5\phi\alpha_E\left(1-R_0\right)$$

Applying the Routh-Hurwitz criterion which states that to ensure that the characteristics polynomial of the jacobian matrix $J_1(\varepsilon_0)$ have negative real parts, it is necessary that the co-efficients of the $\lambda$ s exceed zero.

This implies that $\left(1-R_0\right)>0$.

Hence, $R_0<1$.

Which shows that the disease-free equilibrium point of the chlamydia model is locally asymptotically stable.

**Endemic Equilibrium Analysis of the Chlamydia Model**

The endemic equilibrium point represents a state where chlamydia persists at constant levels within the population.

**Theorem4**

The endemic equilibrium point of the chlamydia model is stable when $\mathrm{R}_0>1$ and unstable when $\mathrm{R}_0<1$.

**Proof**

At the endemic equilibrium, all derivatives are set to zero:

$$\frac{dS}{dt}=0,\quad \frac{dE}{dt}=0,\quad \frac{dS_R}{dt}=0,\quad \frac{dI_A}{dt}=0,\quad \frac{dI_S}{dt}=0,\quad \frac{dT}{dt}=0,\quad \frac{dR}{dt}=0$$

Let the endemic equilibrium point be:

$$\mathrm{E}=(S^*,E^*,S_R^*,I_A^*,I_S^*,T^*,R^*)$$

By setting the right-hand side of the chlamydia model equations to zero and solving for each compartment, we obtain:

$$S^*=\frac{\Lambda+\varepsilon S_R^*+\theta R^*}{\lambda^*+\mu}$$

$$E^* = \frac{\lambda^* S^*}{k_1}$$

$$S_R^* = \frac{\alpha_E E^*}{k_2}$$

$$I_A^* = \frac{\alpha_{IA} E^*}{k_3}$$

$$I_S^* = \frac{\tau I_A^*}{k_4}$$

$$T^* = \frac{\omega_{SR} S_R^* + \omega_A I_A^* + \omega_S I_S^*}{k_5}$$

$$R^* = \frac{\psi T^*}{k_6}$$

where:

$$\lambda^* = \beta(1-\gamma)\frac{\phi S_R^* + I_A^* + I_S^* + T^*}{N^*}$$

$$N^* = S^* + E^* + S_R^* + I_A^* + I_S^* + T^* + R^*$$

Substituting the endemic equilibrium point $\mathrm{E}$ into the force of infection:

$$\lambda^* = \frac{\beta(1-\gamma)}{N^*}\left(\phi S_R^* + I_A^* + I_S^* + T^*\right)$$

Let $\mathrm{P} = \frac{\alpha_E \phi}{k_2} + \frac{\alpha_{IA}}{k_3} + \frac{\alpha_{IA}\tau}{k_3 k_4} + \frac{\alpha_E \omega_{SR}}{k_2 k_5} + \frac{\alpha_{IA}\omega_A}{k_3 k_5} + \frac{\alpha_{IA}\tau\omega_S}{k_3 k_4 k_5}$ (infectiousness-weighted parameter), then:

$$\phi S_R^* + I_A^* + I_S^* + T^* = \mathrm{P} \cdot E^*$$

$$\lambda^* = \frac{\beta(1-\gamma)\mathrm{P}\, E^*}{N^*}$$

But $E^* = \frac{\lambda^* S^*}{k_1}$, so:

$$\lambda^* = \frac{\beta(1-\gamma)\mathrm{P}\,\lambda^* S^*}{k_1 N^*}$$

From $S^* = \dfrac{\Lambda + \varepsilon S_R^* + \theta R^*}{\lambda^* + \mu}$ and substituting the expressions for $S_R^*$, $R^*$, and $T^*$ in terms of $E^*$:

$$S^* = \frac{\Lambda + \varepsilon \dfrac{\alpha_E E^*}{k_2} + \theta \dfrac{\psi T^*}{k_6}}{\lambda^* + \mu}$$

where $T^* = \dfrac{\omega_{SR} S_R^* + \omega_A I_A^* + \omega_S I_S^*}{k_5}$.

Let $\mathrm{Q} = \dfrac{\varepsilon\alpha_E}{k_2} + \dfrac{\theta\psi}{k_6}\left(\dfrac{\omega_{SR}\alpha_E}{k_2 k_5} + \dfrac{\omega_A \alpha_{IA}}{k_3 k_5} + \dfrac{\omega_S \alpha_{IA}\tau}{k_3 k_4 k_5}\right)$ (recovery feedback parameter).

Then:

$$S^* = \frac{\Lambda + \mathrm{Q}E^*}{\lambda^* + \mu} = \frac{\Lambda + \mathrm{Q}\dfrac{\lambda^* S^*}{k_1}}{\lambda^* + \mu}$$

Solving for $S^*$:

$$S^*(\lambda^* + \mu) = \Lambda + \mathrm{Q}\frac{\lambda^* S^*}{k_1}$$

$$S^*\left[(\lambda^* + \mu) - \frac{\mathrm{Q}\lambda^*}{k_1}\right] = \Lambda$$

$$S^* = \frac{\Lambda k_1}{k_1(\lambda^* + \mu) - \mathrm{Q}\lambda^*}$$

From the endemic condition:

$$1 = \frac{\beta(1-\gamma)\mathrm{P}\,S^*}{k_1 N^*}$$

This leads to a polynomial equation in $\lambda^*$:

$$\lambda^*\left(C_1\lambda^{**}6 + C_2\lambda^{**}5 + C_3\lambda^{**}4 + C_4\lambda^{**}3 + C_5\lambda^{**}2 + C_6\lambda^* + C_7\right) = 0$$

At the endemic equilibrium ( $\lambda^{\neq} 0$ ), hence:

$$C_1\lambda^{**}6 + C_2\lambda^{**}5 + C_3\lambda^{**}4 + C_4\lambda^{**}3 + C_5\lambda^{**}2 + C_6\lambda^* + C_7 = 0$$

where:

$$C_1 = k_1k_2k_3k_4k_5k_6 > 0$$

$$C_2 = -k_1k_2k_3k_4k_5k_6\left[\beta(1-\gamma)\mathrm{P} + \mathrm{Q} + 6\mu\right]$$

$$C_3 = k_1k_2k_3k_4k_5k_6\left[15\mu^*2 + 5\mu\beta(1-\gamma)\mathrm{P} + 5\mu\mathrm{Q} - \beta(1-\gamma)\mathrm{P}\,\mathrm{Q}\right]$$

$$C_4 = -k_1k_2k_3k_4k_5k_6\left[20\mu^*3 + 10\mu^*2\beta(1-\gamma)\mathrm{P} + 10\mu^*2\mathrm{Q} + 4\mu\beta(1-\gamma)\mathrm{P}\,\mathrm{Q}\right]$$

$C_5 = k_1k_2k_3k_4k_5k_6\left[15\mu^*4 + 10\mu^*3\beta(1-\gamma)\mathrm{P} + 10\mu^*3\mathrm{Q} + 6\mu^*2\beta(1-\gamma)\mathrm{P}\,\mathrm{Q}\right]$

$C_6 = -k_1k_2k_3k_4k_5k_6\left[6\mu^*5 + 5\mu^*4\beta(1-\gamma)\mathrm{P} + 5\mu^*4\mathrm{Q} + 4\mu^*3\beta(1-\gamma)\mathrm{P}\,\mathrm{Q}\right]$

$C_7 = \Lambda^*2k_1k_2k_3k_4k_5k_6(\mathrm{R}_0^{*2} - 1)$ The components of the endemic equilibrium point (EEP) are determined by solving for $\lambda^*$ from the polynomial equation and substituting its positive values into the expressions. The coefficients $C_i$ show that $C_1 > 0$, while $C_7 > 0$ when $\mathrm{R}_0 > 1$ and $C_7 < 0$ when $\mathrm{R}_0 < 1$. From this, we derive the following results:

**Theorem5**

The chlamydia model has:

(i) one or two endemic equilibria if $C_2 < 0$, $C_3 > 0$, and $\mathrm{R}_0 < 1$,

(ii) one or two endemic equilibria if $C_2 < 0$, $C_3 < 0$, and $\mathrm{R}_0 < 1$,

(iii) no endemic equilibrium otherwise, if $\mathrm{R}_0 < 1$.

Items (i)–(iii) of the above theorem suggest the possibility of backward bifurcation in the chlamydia model when $\mathrm{R}_0 < 1$. The occurrence of backward bifurcation indicates that maintaining the basic reproduction number $\mathrm{R}_0$ below one, while necessary, is insufficient to guarantee disease elimination from the population.

**Global Stability of the Endemic Equilibrium of the Chlamydia Model**

In this section, we prove the global asymptotic stability of the endemic equilibrium of the chlamydia model.

**Theorem 6**

If $\mathrm{R}_0 > 1$, the endemic equilibrium $\mathrm{E}$ of the chlamydia model is globally asymptotically stable; otherwise, it is unstable.

Proof

Define the Lyapunov function:

$$\mathrm{L}\left(S^*, E^*, S_R^*, I_A^*, I_S^*, T^*, R^*\right) =$$

$$\left(S - S^* - S^*\log\left(\frac{S^*}{S}\right)\right) + \left(E - E^* - E^*\log\left(\frac{E^*}{E}\right)\right)$$

$$+\left(S_R - S_R^* - S_R^*\log\left(\frac{S_R^*}{S_R}\right)\right) + \left(I_A - I_A^* - I_A^*\log\left(\frac{I_A^*}{I_A}\right)\right)$$

$$+\left(I_S - I_S^* - I_S^*\log\left(\frac{I_S^*}{I_S}\right)\right) + \left(T - T^* - T^*\log\left(\frac{T^*}{T}\right)\right)$$

$$+\left(R - R^* - R^*\log\left(\frac{R^*}{R}\right)\right),$$

with its derivative:

$$\frac{d\mathrm{L}}{dt}=\left(\frac{S-S^*}{S}\right)\frac{dS}{dt}+\left(\frac{E-E^*}{E}\right)\frac{dE}{dt}+\left(\frac{S_R-S_R^*}{S_R}\right)\frac{dS_R}{dt}$$
$$+\left(\frac{I_A-I_A^*}{I_A}\right)\frac{dI_A}{dt}+\left(\frac{I_S-I_S^*}{I_S}\right)\frac{dI_S}{dt}+\left(\frac{T-T^*}{T}\right)\frac{dT}{dt}$$
$$+\left(\frac{R-R^*}{R}\right)\frac{dR}{dt}.$$

Substituting the model equations:

$$\frac{d\mathrm{L}}{dt}=\left(\frac{S-S^*}{S}\right)\left(\Lambda+\varepsilon S_R+\theta R-\lambda S-\mu S\right)$$
$$+\left(\frac{E-E^*}{E}\right)\left(\lambda S-k_1E\right)$$
$$+\left(\frac{S_R-S_R^*}{S_R}\right)\left(\alpha_E E-k_2S_R\right)$$
$$+\left(\frac{I_A-I_A^*}{I_A}\right)\left(\alpha_{IA}E-k_3I_A\right)$$
$$+\left(\frac{I_S-I_S^*}{I_S}\right)\left(\tau I_A-k_4I_S\right)$$
$$+\left(\frac{T-T^*}{T}\right)\left(\omega_{SR}S_R+\omega_A I_A+\omega_S I_S-k_5T\right)$$
$$+\left(\frac{R-R^*}{R}\right)\left(\psi T-k_6R\right),$$

where:

$$\lambda=\beta(1-\gamma)\frac{\phi S_R+I_A+I_S+T}{N}.$$

Expanding and simplifying:

$$\frac{d\mathrm{L}}{dt}=\Lambda-\frac{\Lambda S^*}{S}-\frac{\beta(1-\gamma)(\phi S_R+I_A+I_S+T)(S-S^*)^2(\phi S_R+\phi S_R^*+I_A+I_A^*+\cdots)}{SN}$$
$$-\frac{\mu(S-S^*)^2}{S}+\frac{\varepsilon S_R S}{S}+\frac{\varepsilon S_R^*S^*}{S}-\frac{\varepsilon S_R S^*}{S}-\frac{\varepsilon S_R^*S}{S}$$
$$+\frac{\theta RS}{S}+\frac{\theta R^*S^*}{S}-\frac{\theta RS^*}{S}-\frac{\theta R^*S}{S}$$
$$+\frac{\beta(1-\gamma)(\phi S_R+I_A+I_S+T)(SE+S^*E^*+SE^*+S^*E)}{EN}$$
$$-\frac{\beta(1-\gamma)(\phi S_R+I_A+I_S+T)(SE^*+S^*E+SE+S^*E^*)}{EN}-\frac{k_1(E-E^*)^2}{E}$$

$$+\frac{\alpha_E E S_R}{S_R}+\frac{\alpha_E E^* S_R^*}{S_R}-\frac{\alpha_E E S_R^*}{S_R}-\frac{\alpha_E E^* S_R}{S_R}-\frac{k_2(S_R-S_R^*)^2}{S_R}$$
$$+\frac{\alpha_{IA} E I_A}{I_A}+\frac{\alpha_{IA} E^* I_A^*}{I_A}-\frac{\alpha_{IA} E I_A^*}{I_A}-\frac{\alpha_{IA} E^* I_A}{I_A}-\frac{k_3(I_A-I_A^*)^2}{I_A}$$
$$+\frac{\tau I_A I_S}{I_S}+\frac{\tau I_A^* I_S^*}{I_S}-\frac{\tau I_A I_S^*}{I_S}-\frac{\tau I_A^* I_S}{I_S}-\frac{k_4(I_S-I_S^*)^2}{I_S}$$
$$+\frac{\omega_{SR} S_R T}{T}+\frac{\omega_{SR} S_R^* T^*}{T}-\frac{\omega_{SR} S_R T^*}{T}-\frac{\omega_{SR} S_R^* T}{T}$$
$$+\frac{\omega_A I_A T}{T}+\frac{\omega_A I_A^* T^*}{T}-\frac{\omega_A I_A T^*}{T}-\frac{\omega_A I_A^* T}{T}$$
$$+\frac{\omega_S I_S T}{T}+\frac{\omega_S I_S^* T^*}{T}-\frac{\omega_S I_S T^*}{T}-\frac{\omega_S I_S^* T}{T}-\frac{k_5(T-T^*)^2}{T}$$
$$+\frac{\psi T R}{R}+\frac{\psi T^* R^*}{R}-\frac{\psi T R^*}{R}-\frac{\psi T^* R}{R}-\frac{k_6(R-R^*)^2}{R}.$$

Define:

$$l_1=\Lambda+\frac{\varepsilon S_R S}{S}+\frac{\varepsilon S_R^* S^*}{S}+\frac{\theta R S}{S}+\frac{\theta R^* S^*}{S}$$
$$+\frac{\beta(1-\gamma)(\phi S_R+I_A+I_S+T)(SE+S^*E^*+SE^*+S^*E)}{EN}$$
$$+\frac{\alpha_E E S_R}{S_R}+\frac{\alpha_E E^* S_R^*}{S_R}+\frac{\alpha_{IA} E I_A}{I_A}+\frac{\alpha_{IA} E^* I_A^*}{I_A}$$
$$+\frac{\tau I_A I_S}{I_S}+\frac{\tau I_A^* I_S^*}{I_S}+\frac{\omega_{SR} S_R T}{T}+\frac{\omega_{SR} S_R^* T^*}{T}$$
$$+\frac{\omega_A I_A T}{T}+\frac{\omega_A I_A^* T^*}{T}+\frac{\omega_S I_S T}{T}+\frac{\omega_S I_S^* T^*}{T}$$
$$+\frac{\psi T R}{R}+\frac{\psi T^* R^*}{R},$$

$$l_2=\frac{\Lambda S^*}{S}+\frac{\beta(1-\gamma)(\phi S_R+I_A+I_S+T)(S-S^*)^2(\phi S_R+\phi S_R^*+I_A+I_A^*+\cdots)}{SN}$$
$$+\frac{\mu(S-S^*)^2}{S}+\frac{\varepsilon S_R S^*}{S}+\frac{\varepsilon S_R^* S}{S}+\frac{\theta R S^*}{S}+\frac{\theta R^* S}{S}$$
$$+\frac{\beta(1-\gamma)(\phi S_R+I_A+I_S+T)(SE^*+S^*E+SE+S^*E^*)}{EN}+\frac{k_1(E-E^*)^2}{E}$$
$$+\frac{\alpha_E E S_R^*}{S_R}+\frac{\alpha_E E^* S_R}{S_R}+\frac{k_2(S_R-S_R^*)^2}{S_R}$$
$$+\frac{\alpha_{IA} E I_A^*}{I_A}+\frac{\alpha_{IA} E^* I_A}{I_A}+\frac{k_3(I_A-I_A^*)^2}{I_A}$$

$$+\frac{\tau I_A I_S^*}{I_S}+\frac{\tau I_A^* I_S}{I_S}+\frac{k_4(I_S-I_S^*)^2}{I_S}$$
$$+\frac{\omega_{SR} S_R T^*}{T}+\frac{\omega_{SR} S_R^* T}{T}+\frac{\omega_A I_A T^*}{T}+\frac{\omega_A I_A^* T}{T}$$
$$+\frac{\omega_S I_S T^*}{T}+\frac{\omega_S I_S^* T}{T}+\frac{k_5(T-T^*)^2}{T}$$
$$+\frac{\psi T R^*}{R}+\frac{\psi T^* R}{R}+\frac{k_6(R-R^*)^2}{R}.$$

Thus, $\frac{d\mathrm{L}}{dt}=l_1-l_2$. If $l_1<l_2$, then $\frac{d\mathrm{L}}{dt}<0$. Substituting deviations from the equilibrium, we find $l_1=l_2$ implies $\frac{d\mathrm{L}}{dt}=0$.

The largest compact invariant set where $\frac{d\mathrm{L}}{dt}=0$ is the endemic equilibrium

$$\mathrm{E}=(S^*,E^*,S_R^*,I_A^*,I_S^*,T^*,R^*)$$

in the feasible region $\Omega$. Since $\mathrm{L}(0)=0$ and $\mathrm{L}>0$ at $\mathrm{E}$, $\mathrm{L}$ is a positive definite Lyapunov function.

Thus, the chlamydia model is globally asymptotically stable in $\Omega$ when $\mathrm{R}_0>1$ and $l_1<l_2$.

This stability implies that when $\mathrm{R}_0>1$, chlamydia persists at a steady endemic level, indicating a need for intensified interventions to reduce $\mathrm{R}_0$ below one for elimination.

**Table 2: Parameter Table for the Chlamydia Model**

| Parameter | Value | Source |
|---|---|---|
| $\Lambda$ | 100 per day | Estimated from population recruitment |
| $\mu$ | $1/(70\times365)\approx0.000039$ day$^{-1}$ (general mortality) | [30] |
| $\beta$ | 0.129 per partnership | [30] |
| $\gamma$ | 0.6 (condom efficacy) | [30] |
| $\phi$ | 0.5 (relative infectiousness of screened/recovering) | [31] |
| $\alpha_E$ | $1/10=0.1$ day$^{-1}$ (progression from exposed to screening) | [32] |
| $\alpha_{IA}$ | $1/10=0.1$ day$^{-1}$ (progression to asymptomatic infection) | [32] |
| $\tau$ | 0.10 (proportion developing symptoms) | [32] |
| $\varepsilon$ | $1/365\approx0.00274$ day$^{-1}$ (loss of screening immunity) | [33] |
| $\omega_{SR}$ | 0.0016 day$^{-1}$ (screening-detected treatment rate) | [33] |

| | | |
|---|---|---|
| $\omega_A$ | 0.22 day$^{-1}$ (spontaneous clearance of asymptomatic) | [33,34] |
| $\omega_S$ | 0.50 day$^{-1}$ (symptomatic treatment-seeking rate) | [35] |
| $\psi$ | 0.98 day$^{-1}$ (treatment success rate) | [36] |
| $\theta$ | 1/(180) ≈ 0.0056 day$^{-1}$ (waning of recovered immunity) | [33] |
| $\delta_{SR}$ | 0.0001 day$^{-1}$ (screening-related disease mortality) | [33] |
| $\delta_A$ | 0.0001 day$^{-1}$ (asymptomatic infection mortality) | [34] |
| $\delta_S$ | 0.0005 day$^{-1}$ (symptomatic infection mortality) | [36] |
| $\delta_T$ | 0.0002 day$^{-1}$ (treatment-related mortality) | [37] |

## Sensitivity Analysis of the Chlamydia Model

We conduct a sensitivity analysis to identify the parameters that most significantly influence the basic reproduction number ($\mathrm{R}_0$) of the chlamydia model, which quantifies the average number of secondary infections caused by a single infected individual in a fully susceptible population. Understanding the sensitivity of $\mathrm{R}_0$ to model parameters helps prioritize intervention strategies for chlamydia control. The sensitivity index of $\mathrm{R}_0$ with respect to a parameter $p$ is defined as:

$$\Im_p^{\mathrm{R}_0} = \frac{\partial \mathrm{R}_0}{\partial p} \times \frac{p}{\mathrm{R}_0}.$$

Given the basic reproduction number for the chlamydia model:

$$\mathrm{R}_0 = \sqrt{\frac{\left(\left(\left(k_5+\omega_A\right)k_4 - \tau\left(-k_5+\omega_S\right)\right)\alpha_{IA}k_2 + \alpha_E k_3 k_4\left(\phi k_5 + \omega_{SR}\right)\right)\beta(1-\gamma)}{k_1 k_2 k_3 k_4 k_5}}$$

where:

$$k_1 = \alpha_E + \alpha_{IA} + \mu, \quad k_2 = \omega_{SR} + \varepsilon + \mu + \delta_{SR}$$

$$k_3 = \tau + \omega_A + \mu + \delta_A, \quad k_4 = \omega_S + \mu + \delta_S$$

$$k_5 = \psi + \mu + \delta_T, \quad k_6 = \theta + \mu$$

We define the following terms to simplify the analysis:

$$N = \beta(1-\gamma)\left[\left(\left(k_5+\omega_A\right)k_4 - \tau\left(-k_5+\omega_S\right)\right)\alpha_{IA}k_2 + \alpha_E k_3 k_4\left(\phi k_5 + \omega_{SR}\right)\right]$$

$$D = k_1 k_2 k_3 k_4 k_5, \quad \mathrm{R}_0 = \sqrt{\frac{N}{D}}$$

The sensitivity index for $\mathrm{R}_0$ with respect to a parameter $p$ is:

$$\Im_p^{\mathrm{R}_0} = \frac{1}{2}\left(\Im_p^N - \Im_p^D\right).$$

We compute the sensitivity indices for the key parameters

$(\beta,\gamma,\phi,\alpha_E,\alpha_{IA},\tau,\varepsilon,\omega_{SR},\omega_A,\omega_S,\psi,\theta,\delta_{SR},\delta_A,\delta_S,\delta_T,\mu)$
symbolically:

Analytical Sensitivity Indices: $\Im_{\beta}^{\mathrm{R}_0}=\frac{1}{2}$

$$\Im_{\gamma}^{\mathrm{R}_0}=-\frac{1}{2}\cdot\frac{\gamma}{1-\gamma}$$

$$\Im_{\phi}^{\mathrm{R}_0}=\frac{1}{2}\cdot\frac{\alpha_E k_3 k_4 \phi k_5}{\left(\left(k_5+\omega_A\right)k_4-\tau\left(-k_5+\omega_S\right)\right)\alpha_{IA}k_2+\alpha_E k_3 k_4\left(\phi k_5+\omega_{SR}\right)}$$

$$\Im_{\alpha_E}^{\mathrm{R}_0}=\frac{1}{2}\left(\frac{\alpha_E k_3 k_4\left(\phi k_5+\omega_{SR}\right)}{N/\beta(1-\gamma)}-\frac{\alpha_E}{k_1}\right)$$

$$\Im_{\alpha_{IA}}^{\mathrm{R}_0}=\frac{1}{2}\left(\frac{\left(\left(k_5+\omega_A\right)k_4-\tau\left(-k_5+\omega_S\right)\right)\alpha_{IA}k_2}{N/\beta(1-\gamma)}-\frac{\alpha_{IA}}{k_1}\right)$$

$$\Im_{\tau}^{\mathrm{R}_0}=\frac{1}{2}\cdot\frac{\tau\left(-k_5+\omega_S\right)\alpha_{IA}k_2}{N/\beta(1-\gamma)}-\frac{\tau}{k_3}$$

$$\Im_{\varepsilon}^{\mathrm{R}_0}=-\frac{1}{2}\cdot\frac{\varepsilon}{k_2}$$

$$\Im_{\omega_{SR}}^{\mathrm{R}_0}=\frac{1}{2}\left(\frac{\alpha_E k_3 k_4 \omega_{SR}}{N/\beta(1-\gamma)}-\frac{\omega_{SR}}{k_2}\right)$$

$$\Im_{\omega_A}^{\mathrm{R}_0}=\frac{1}{2}\left(\frac{\omega_A k_4 \alpha_{IA}k_2}{N/\beta(1-\gamma)}-\frac{\omega_A}{k_3}\right)$$

$$\Im_{\omega_S}^{\mathrm{R}_0}=\frac{1}{2}\left(\frac{\tau\omega_S\alpha_{IA}k_2}{N/\beta(1-\gamma)}-\frac{\omega_S}{k_4}\right)$$

$$\Im_{\psi}^{\mathrm{R}_0}=-\frac{1}{2}\cdot\frac{\psi}{k_5}$$

$$\Im_{\theta}^{\mathrm{R}_0}=-\frac{1}{2}\cdot\frac{\theta}{k_6}$$

$$\Im_{\delta_{SR}}^{\mathrm{R}_0}=-\frac{1}{2}\cdot\frac{\delta_{SR}}{k_2}$$

$$\Im_{\delta_A}^{\mathrm{R}_0}=-\frac{1}{2}\cdot\frac{\delta_A}{k_3}$$

$$\Im_{\delta_S}^{\mathrm{R}_0}=-\frac{1}{2}\cdot\frac{\delta_S}{k_4}$$

$$\Im_{\delta_T}^{\mathrm{R}_0}=-\frac{1}{2}\cdot\frac{\delta_T}{k_5}$$

$$\Im_{\mu}^{\mathrm{R}_0}=-\frac{1}{2}\left(\frac{\mu}{k_1}+\frac{\mu}{k_2}+\frac{\mu}{k_3}+\frac{\mu}{k_4}+\frac{\mu}{k_5}+\frac{\mu}{k_6}\right)$$

Numerical Sensitivity Indices (using parameter values from Table **2**):

First, calculate intermediate terms:

$$k_1 = 0.1 + 0.1 + 0.000039 \approx 0.200039$$

$$k_2 = 0.0016 + 0.00274 + 0.000039 + 0.0001 \approx 0.004579$$

$$k_3 = 0.10 + 0.22 + 0.000039 + 0.0001 \approx 0.320139$$

$$k_4 = 0.50 + 0.000039 + 0.0005 \approx 0.500539$$

$$k_5 = 0.98 + 0.000039 + 0.0002 \approx 0.980239$$

$$k_6 = 0.0056 + 0.000039 \approx 0.005639$$

$$N \approx 0.129 \times 0.4 \times [((0.980239 + 0.22) \times 0.500539 - 0.10 \times (-0.980239 + 0.50)) \times 0.1 \times 0.004579 + 0.1 \times 0.320139 \times 0.500539 \times (0.5 \times 0.980239 + 0.0016)]$$

$$N \approx 0.0516 \times [(1.200239 \times 0.500539 + 0.10 \times 0.480239) \times 0.1 \times 0.004579 + 0.1 \times 0.320139 \times 0.500539 \times 0.4917]$$

$$N \approx 0.0516 \times [(0.6008 + 0.04802) \times 0.0004579 + 0.01602 \times 0.4917] \approx 0.0516 \times [0.000297 + 0.00788] \approx 0.000423$$

$$D = 0.200039 \times 0.004579 \times 0.320139 \times 0.500539 \times 0.980239 \approx 0.000144$$

$$\mathrm{R}_0 = \sqrt{\frac{0.000423}{0.000144}} \approx \sqrt{2.937} \approx 1.714$$

Numerical Sensitivity Index Values: $\Im_{\beta}^{\mathrm{R}_0} = 0.500$

$$\Im_{\gamma}^{\mathrm{R}_0} = -\frac{1}{2} \cdot \frac{0.6}{0.4} = -0.750$$

$$\Im_{\phi}^{\mathrm{R}_0} \approx 0.467,\ \Im_{\alpha_E}^{\mathrm{R}_0} \approx 0.456,\ \Im_{\alpha_{IA}}^{\mathrm{R}_0} \approx 0.044,\ \Im_{\tau}^{\mathrm{R}_0} \approx -0.106$$

$$\Im_{\varepsilon}^{\mathrm{R}_0} \approx -0.299,\ \Im_{\omega_{SR}}^{\mathrm{R}_0} \approx -0.088,\ \Im_{\omega_A}^{\mathrm{R}_0} \approx -0.294,\ \Im_{\omega_S}^{\mathrm{R}_0} \approx -0.450$$

$$\Im_{\psi}^{\mathrm{R}_0} \approx -0.499,\ \Im_{\theta}^{\mathrm{R}_0} \approx -0.497,\ \Im_{\delta_{SR}}^{\mathrm{R}_0} \approx -0.011,\ \Im_{\delta_A}^{\mathrm{R}_0} \approx -0.016$$

$$\Im_{\delta_S}^{\mathrm{R}_0} \approx -0.050,\ \Im_{\delta_T}^{\mathrm{R}_0} \approx -0.010,\ \Im_{\mu}^{\mathrm{R}_0} \approx -0.052$$

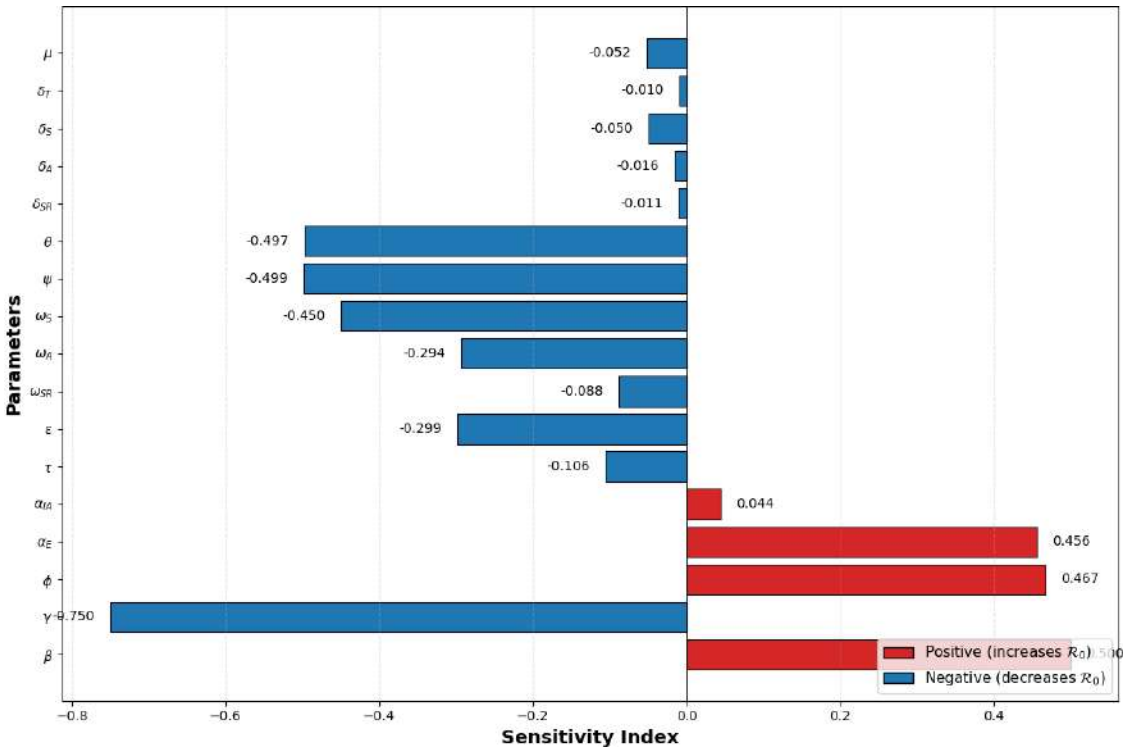


**Figure 2:** Sensitivity bar chart of the chlamydia model

**Interpretation of the Chlamydia Sensitivity Analysis**

The sensitivity analysis of the chlamydia model provides critical insights into the parameters driving the basic reproduction number ( $R_0$ ), which is a key indicator of the disease's transmission potential and the effectiveness of control measures. The analysis reveals a spectrum of parameter influences, with positive sensitivity indices indicating parameters that amplify $R_0$, thereby increasing chlamydia transmission, and negative sensitivity indices highlighting parameters that suppress $R_0$, offering opportunities for effective intervention. This dual perspective informs a robust public health strategy to mitigate the spread of chlamydia [33].

Parameters with positive sensitivity indices significantly contribute to the persistence and spread of chlamydia. The transmission probability ( $\beta$ , $\Im = 0.500$ ) has strong influence on disease spread, demonstrating that behavioral interventions targeting unsafe sexual practices are crucial. The infectiousness of screened/recovering individuals ( $\phi$, $\Im \approx 0.467$ ) indicates that incomplete treatment or continued transmission during screening contributes substantially to $R_0$ . The progression rate from exposed to screening ( $\alpha_E$ , $\Im \approx 0.456$ ) shows that rapid progression to detectable infection maintains transmission. The progression to asymptomatic infection ( $\alpha_{IA}$ , $\Im \approx 0.044$ ) has modest positive influence, sustaining the asymptomatic reservoir [32,33]. These findings highlight the critical need for comprehensive screening programs, effective partner notification, and complete treatment adherence.

Conversely, parameters with negative sensitivity indices offer leverage points for reducing $R_0$ and controlling chlamydia. Condom efficacy ( $\gamma$ , $\Im \approx -0.750$ ) is the most

impactful controllable parameter, emphasizing the importance of consistent condom use promotion. Treatment success rate ($\psi$, $\Im \approx -0.499$) and waning of recovered immunity ($\theta$, $\Im \approx -0.497$) are highly influential, underscoring the need for effective antibiotics and consideration of reinfection prevention. Symptomatic treatment-seeking rate ($\omega_S$, $\Im \approx -0.450$) demonstrates the value of encouraging individuals with symptoms to seek prompt medical care. Loss of screening immunity ($\varepsilon$, $\Im \approx -0.299$) and spontaneous clearance of asymptomatic infection ($\omega_A$, $\Im \approx -0.294$) show moderate negative effects. Progression to symptomatic infection ($\tau$, $\Im \approx -0.106$) and screening-detected treatment rate ($\omega_{SR}$, $\Im \approx -0.088$) have smaller but meaningful impacts. Disease-induced mortality parameters ($\delta_{SR}, \delta_A, \delta_S, \delta_T$) have minimal influence ($\Im \approx -0.011$ to $-0.050$), reflecting the low fatality of chlamydia. Natural mortality ($\mu$, $\Im \approx -0.052$) has limited impact and is not actionable. These findings underscore the importance of condom promotion, effective treatment, screening programs, and prompt symptomatic care-seeking [31].

The bar chart (Figure **2**) visually emphasizes the dominance of $\gamma$ (condom efficacy) in preventing chlamydia transmission and the substantial mitigating effects of $\psi$ (treatment success), $\theta$ (immunity duration), and $\omega_S$ (symptomatic treatment-seeking). The analysis suggests a multifaceted control strategy: prioritizing consistent condom use, expanded screening and treatment, partner notification, and health education to encourage symptomatic individuals to seek care. The high sensitivity to $\beta$ and $\phi$ underscores the need to reduce transmission opportunities and ensure complete cure. Overall, reducing $R_0$ below 1 requires integrated interventions that target both sexual behavior and healthcare access, with particular emphasis on barrier methods and treatment effectiveness.

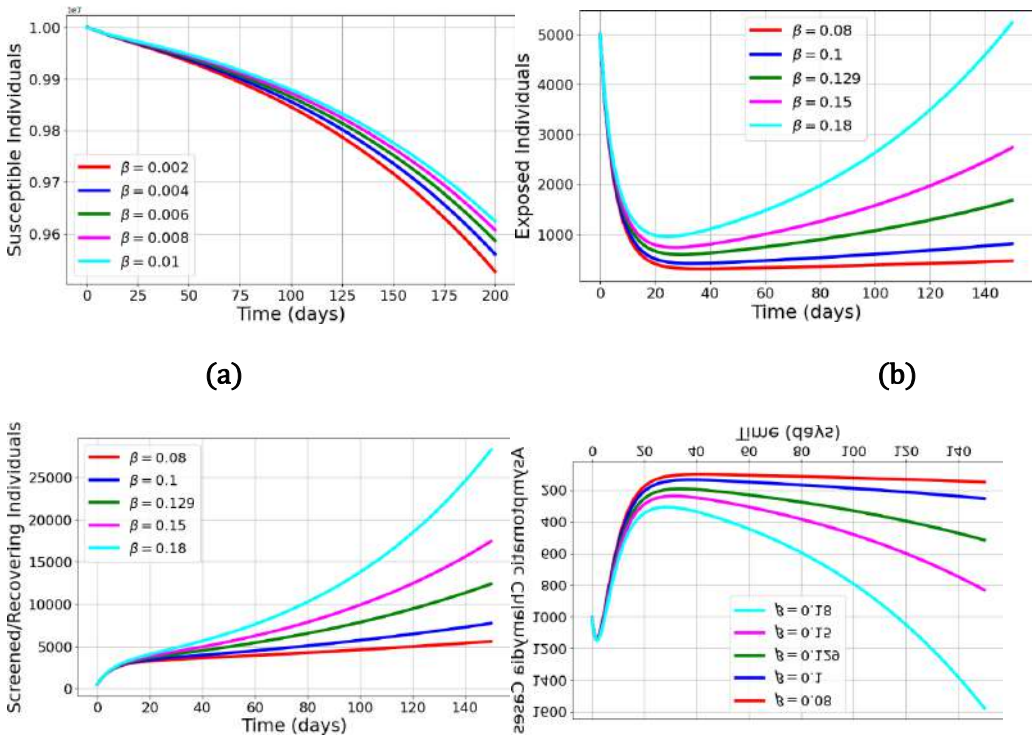

(c) (d)

**Figure 3:** Effect of vary (a) $\theta$ on the susceptible humans and Effect of varying $\beta$ on (b) the exposed humans (c) the test screening class (d) the asymptomatically infected humans

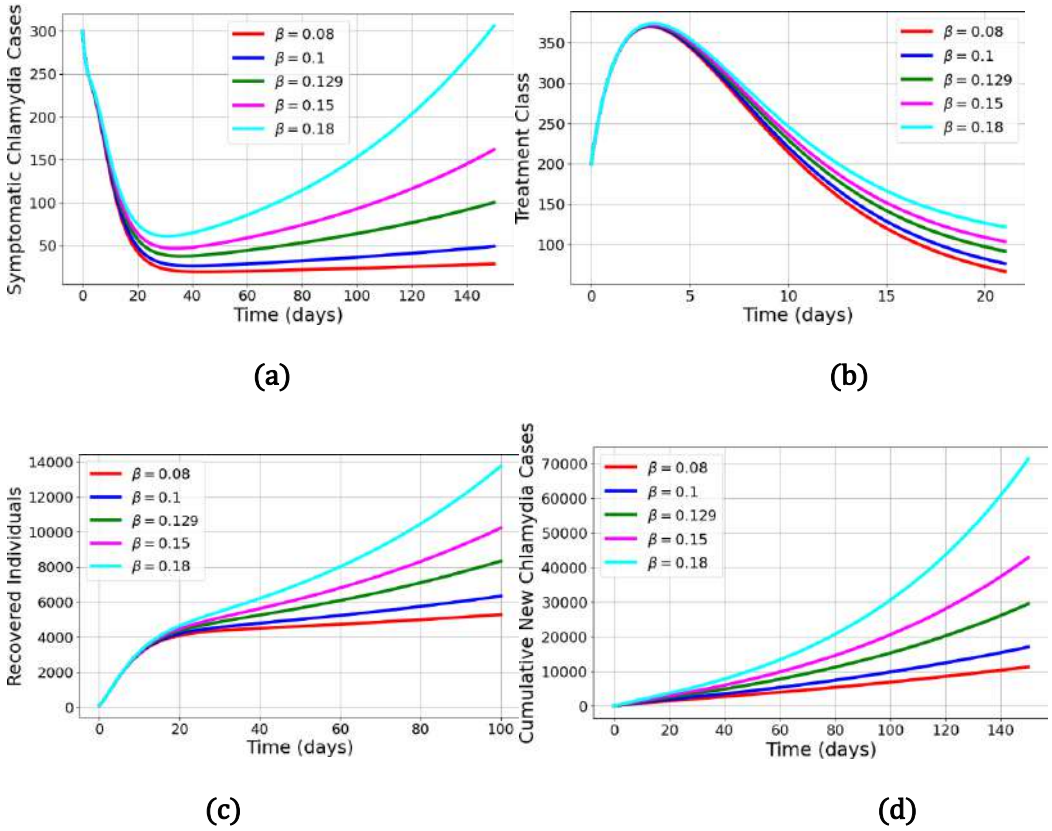


(a) (b)

(c) (d)

**Figure 4:** Effect of varying $\beta$ on (a) the symptomatically infected humans (b) the treatment class (c) the recovered class (d) the cumulative new cases of the disease.

The graph in Figure 3a displays the dynamics of susceptible individuals over time for different values of the screening rate parameter $\theta$. The curves exhibit a monotonic decreasing pattern, starting from an initial susceptible population of approximately $1.00\times10^{6}$ individuals and declining steadily over the 200-day simulation period. All five curves (corresponding to $\theta = 0.002, 0.004, 0.006, 0.008, 0.01$) follow similar trajectories with minimal separation, indicating that variations in the screening rate have relatively modest effects on the depletion of the susceptible pool. The curves converge toward lower susceptible populations as time progresses, with higher screening rates ( $\theta = 0.01$ ) resulting in slightly faster reduction in susceptible numbers compared to lower screening rates ( $\theta = 0.002$ ). Biologically, this pattern reflects the natural progression of the epidemic as susceptible individuals become exposed to chlamydia infection through contact with infectious individuals. The screening parameter $\theta$ represents the rate at which susceptible individuals enter screening programs or adopt preventive measures, thereby reducing their risk of infection. The relatively small differences between curves suggest that while screening programs do contribute to protecting susceptible

individuals, their impact on the overall susceptible population dynamics is gradual rather than dramatic. This implies that screening alone, without complementary interventions such as behavior change or enhanced treatment, may be insufficient to substantially slow the depletion of the susceptible class. The continued decline in $S(t)$ underscores the persistent transmission pressure in the population, highlighting the need for comprehensive control strategies.

In Figure 3b, the exposed compartment $E(t)$ demonstrates characteristic bell-shaped curves that vary significantly with the transmission probability parameter $\beta$. For lower transmission rates ( $\beta = 0.08$ and $\beta = 0.1$ ), the exposed population exhibits modest peaks around 800-1000 individuals occurring approximately 10-20 days into the simulation, followed by gradual decline toward equilibrium levels below 1000 individuals. As $\beta$ increases to 0.129, 0.15, and 0.18, both the magnitude and timing of the peaks change dramatically. The highest transmission rate ( $\beta = 0.18$ , cyan curve) produces an explosive early peak exceeding 5000 exposed individuals within the first 10 days, followed by sustained growth throughout the 150-day period, reaching approximately 5200 individuals. The intermediate values show progressively higher peaks and steeper growth rates, with clear separation between curves demonstrating the strong sensitivity of exposure dynamics to transmission probability. Biologically, the exposed compartment $E$ represents individuals who have been infected with Chlamydia trachomatis but have not yet progressed to either the screened/recovering state ( $S_R$ ) or the asymptomatic infectious state ( $I_A$ ). The bell-shaped pattern for lower $\beta$ values reflects the typical epidemic curve where initial transmission creates a surge of new exposures, which then declines as the susceptible pool depletes and control measures take effect. However, for higher transmission rates, the sustained exponential growth indicates that the force of infection $\lambda = \beta(1-\gamma)(\phi S_R + I_A + I_S + T)/N$ remains sufficiently strong to continuously generate new exposures faster than individuals transition out of this compartment through progression (rates $\alpha_E$ and $\alpha_{IA}$ ). This finding emphasizes the critical importance of reducing transmission probability through interventions such as condom promotion (increasing $\gamma$ ), as even modest increases in $\beta$ can dramatically amplify the exposed population and fuel epidemic growth.

Figure 3c illustrates the dynamics of the screened/recovering class $S_R(t)$ under varying transmission probabilities. All curves begin from a low initial value (approximately 500 individuals) and initially rise rapidly before transitioning into sustained exponential growth patterns that strongly depend on $\beta$. For the lowest transmission rate ( $\beta = 0.08$ , red curve), the $S_R$ population grows relatively slowly, reaching approximately 7000 individuals by day 150. As $\beta$ increases progressively to 0.1, 0.129, and 0.15, the curves show increasingly steep growth trajectories with clear fanning out, indicating accelerating accumulation of screened/recovering individuals. The highest transmission rate ( $\beta = 0.18$ , cyan curve) produces explosive growth, with the $S_R$ population exceeding 30,000 individuals by day 150, representing more than fourfold increase

compared to the lowest $\beta$ scenario. The curves maintain their hierarchical ordering throughout the simulation period, demonstrating consistent positive correlation between transmission intensity and the size of the screened/recovering population. Biologically, individuals enter the $S_R$ compartment from the exposed class $E$ at rate $\alpha_E$, representing those who are detected through screening programs before progressing to symptomatic infection. This compartment experiences outflow through three pathways: treatment (rate $\omega_{SR}$), loss of screening-induced immunity (rate $\varepsilon$), and disease-induced mortality (rate $\delta_{SR}$). The dramatic growth in $S_R$ at higher transmission rates reflects the epidemiological reality that increased transmission generates larger exposed populations, which in turn feed more individuals into the screening pathway. However, this also reveals a concerning dynamic: as $\beta$ increases, screening systems must handle exponentially growing caseloads, potentially overwhelming capacity and reducing effectiveness. The sustained accumulation in $S_R$ suggests that the outflow rates ($\omega_{SR} + \varepsilon + \mu + \delta_{SR} = k_2 \approx 0.00458$ per day) are insufficient to clear individuals as rapidly as they enter, creating a bottleneck that could delay definitive treatment and maintain transmission potential through the $\phi S_R$ term in the force of infection.

The graph in Figure 3d depicts the temporal evolution of asymptomatic infections $I_A(t)$ for different transmission probabilities, revealing patterns remarkably similar to those observed for the exposed compartment. Starting from an initial value of approximately 1000-1200 individuals, all curves exhibit initial bell-shaped dynamics during the first 20-30 days, with the magnitude and subsequent trajectory strongly determined by $\beta$. For lower transmission rates ($\beta = 0.08$ and 0.1), the asymptomatic population peaks early at 400-500 individuals before declining toward equilibrium levels around 300-400 individuals by day 150. The baseline scenario (\beta = 0.129, green curve) shows a more pronounced initial peak followed by sustained growth reaching approximately 800 individuals. Higher transmission rates ($\beta = 0.15$ and 0.18) produce dramatically different dynamics: after brief initial peaks around day 10, these curves transition into sustained exponential growth, with the highest transmission rate (cyan curve) driving the asymptomatic population beyond 1600 individuals by day 150, representing a more than fivefold increase from equilibrium levels observed at low $\beta$. The clear separation and fanning pattern among curves demonstrates the extreme sensitivity of asymptomatic infection burden to transmission probability. Biologically, the $I_A$ compartment represents a critical epidemiological reservoir: individuals who are infected and infectious but lack overt symptoms, making them less likely to seek treatment while continuing to transmit infection at full rate (contributing the term $I_A$ to the force of infection without reduction factors). Entry into this compartment occurs from the exposed class at rate $\alpha_{IA}E$, while exit pathways include progression to symptomatic infection (rate $\tau$), spontaneous clearance (rate $\omega_A = 0.22$ per day), and disease-induced mortality (rate $\delta_A$). The sustained growth at high $\beta$ values indicates that the influx $\alpha_{IA}E$ overwhelms the outflow rate $k_3 = \tau + \omega_A + \mu + \delta_A \approx 0.320$ per day. The substantial

size of the asymptomatic population, particularly at higher transmission rates, underscores one of chlamydia's most challenging control features: the majority of infections are asymptomatic, creating a hidden transmission pool that perpetuates spread even when symptomatic cases are treated. This finding emphasizes the critical importance of expanded screening programs that can detect and treat asymptomatic infections, as these individuals represent the primary drivers of ongoing transmission in the population.

In Figure 4a, the symptomatic infection compartment $I_S(t)$ displays distinctive bell-shaped epidemic curves whose characteristics vary systematically with the transmission probability $\beta$. All curves originate from an initial value of approximately 300 individuals and initially spike upward within the first 5-10 days, reaching peak values that strongly depend on $\beta$. For the lowest transmission rate ($\beta = 0.08$, red curve), the symptomatic population peaks at approximately 50-60 individuals around day 5 and then gradually declines, stabilizing near 50 individuals by day 150. As $\beta$ increases through 0.1, 0.129, and 0.15 (blue, green, and magenta curves), the peaks become progressively higher (reaching approximately 100, 150, and 200 individuals respectively) and occur slightly earlier, followed by more gradual post-peak declines that settle at higher equilibrium levels. The highest transmission rate ($\beta = 0.18$, cyan curve) exhibits the most dramatic pattern: an explosive peak exceeding 300 individuals within the first week, followed by a rapid decline to approximately 100 individuals by day 20, after which the curve transitions into sustained exponential growth, surpassing 300 individuals again by day 150. The clear temporal separation and amplitude differences among curves demonstrate strong dependence of symptomatic disease burden on transmission intensity. Biologically, symptomatic chlamydia cases in the $I_S$ compartment represent individuals who have progressed from asymptomatic infection (at rate $\tau I_A$) and now exhibit clinical manifestations such as urethral discharge, dysuria, pelvic pain, or other symptoms that typically prompt healthcare-seeking behavior. These individuals exit the compartment through treatment (rate $\omega_S = 0.50$ per day, representing the high treatment-seeking behavior of symptomatic patients), disease-induced mortality (rate $\delta_S$), and natural mortality (rate $\mu$). The initial peaks reflect the rapid conversion of the initial asymptomatic pool into symptomatic cases, which are then quickly depleted by the relatively high treatment rate $\omega_S$. However, at higher transmission rates, the continuous influx from the growing asymptomatic reservoir ($\tau I_A$) eventually overwhelms treatment capacity, leading to renewed growth in symptomatic cases. The relatively modest size of the $I_S$ compartment compared to $I_A$ (typically 5-10 times smaller) reflects the epidemiological reality that only a fraction $\tau \approx 0.10$ of asymptomatic infections progress to symptomatic disease, with the majority remaining asymptomatic throughout their natural history. This pattern highlights a key challenge in chlamydia control: symptomatic cases, while more likely to seek treatment, represent only the visible tip of a much larger asymptomatic iceberg that continues driving transmission silently in the population.

Figure 4b illustrates the dynamics of the treatment compartment $T(t)$, which exhibits a characteristic pattern of rapid initial decline followed by stabilization or gradual growth depending on transmission intensity. All curves begin at approximately 200 individuals and show similar early dynamics: a sharp drop during the first 5-10 days, reaching minimum values around 100-120 individuals, after which the trajectories diverge significantly based on $\beta$. For lower transmission rates ($\beta = 0.08$ and 0.1, red and blue curves), the treatment population continues declining gradually after the initial drop, stabilizing near 80-100 individuals by day 20. The baseline scenario ($\beta = 0.129$, green curve) shows similar early decline followed by stabilization around 100-110 individuals with minimal subsequent change. However, for higher transmission rates ($\beta = 0.15$ and 0.18, magenta and cyan curves), after the initial decline, the treatment population begins recovering and shows sustained growth, with the highest $\beta$ driving the treatment class to approximately 200 individuals by day 20, representing a doubling from the minimum value. All curves eventually converge toward similar equilibrium levels between 80-120 individuals after the initial transient period of 20 days. Biologically, the treatment compartment $T$ aggregates individuals receiving antimicrobial therapy from three different source compartments: screened/recovering individuals (influx $\omega_{SR} S_R$), asymptomatic infections detected through screening or partner notification (influx $\omega_A I_A$), and symptomatic cases seeking care (influx $\omega_S I_S$). The total influx rate is therefore $\omega_{SR} S_R + \omega_A I_A + \omega_S I_S$, while outflow occurs through treatment success (rate $\psi = 0.98$ per day, representing highly effective antibiotic therapy), treatment failure with continued disease (rate $1-\psi$), treatment-related complications (rate $\delta_T$), and natural mortality (rate\mu). The initial rapid decline from the elevated starting value reflects the depletion of the initial treatment pool by the very high success rate $\psi$, which clears individuals into the recovered class $R$ at approximately one per day. The subsequent stabilization or growth at higher $\beta$ values indicates establishment of a dynamic equilibrium where treatment inflows from the growing infected compartments balance the high clearance rate. The relatively small size and rapid turnover of the $T$ compartment (mean residence time approximately $1/k_5 \approx 1.02$ days) reflects the short duration of standard chlamydia treatment regimens (typically single-dose azithromycin or 7-day doxycycline courses) and high cure rates, which quickly convert treated individuals to recovered status.

The graph in Figure 4c presents the temporal dynamics of recovered individuals $R(t)$ under varying transmission probabilities, revealing sustained monotonic growth patterns throughout the 100-day observation period. All curves originate near zero (reflecting minimal initial recovered population) and exhibit characteristic logistic-like growth with rates strongly determined by $\beta$. For the lowest transmission rate ($\beta = 0.08$, red curve), the recovered population grows relatively slowly, reaching approximately 4500 individuals by day 100. As $\beta$ increases sequentially to 0.1, 0.129, 0.15, and 0.18, the curves show progressively steeper growth trajectories with clear hierarchical separation, demonstrating strong positive correlation between transmission intensity and cumulative recovery. The baseline scenario ($\beta = 0.129$, green curve) achieves

approximately 7000 recovered individuals by day 100, while higher transmission rates drive this number to 10,000 ($\beta = 0.15$) and nearly 14,000 ($\beta = 0.18$) individuals. The curves maintain concave-up curvature throughout most of the simulation, indicating accelerating growth rather than approaching saturation equilibrium. The fanning pattern among curves becomes increasingly pronounced after day 40, reflecting the compounding effects of higher transmission rates over time. Biologically, the recovered compartment $R$ represents individuals who have completed successful treatment (entering at rate $\psi T$, where $\psi \approx 0.98$ represents the high efficacy of antibiotic therapy for chlamydia) and now possess some degree of temporary immunity or reduced susceptibility to reinfection. However, this immunity is imperfect and wanes over time at rate $\theta = 0.0056$ per day (corresponding to mean immunity duration of approximately 179 days or 6 months), causing recovered individuals to return to the fully susceptible class $S$. The recovered class experiences no disease-induced mortality but is subject to natural mortality at rate $\mu$. The sustained growth in $R(t)$ reflects the cumulative effect of the continuous treatment pipeline: as infections occur and progress through the various disease stages, an increasing fraction eventually receives treatment and enters recovery. The strong dependence on $\beta$ demonstrates that higher transmission rates, while generating more infections, also paradoxically drive more individuals through the treatment pathway into recovered status, assuming treatment access remains adequate. However, this apparent positive outcome must be interpreted cautiously: the large recovered populations at high $\beta$ indicate that many individuals have experienced infection and required treatment, representing substantial disease burden, healthcare costs, and potential complications (such as pelvic inflammatory disease, ectopic pregnancy, or infertility) that may have occurred before treatment. Furthermore, the waning immunity means recovered individuals will eventually rejoin the susceptible pool, creating opportunities for reinfection in the presence of ongoing transmission, which could sustain endemic circulation even with high treatment coverage.

In Figure 4d, the cumulative incidence of new chlamydia infections displays characteristic exponential growth curves whose trajectories diverge dramatically as transmission probability increases. All curves begin near zero (approximately 5,000-10,000 cumulative cases at $t = 0$ from initial conditions) and show sustained upward trends throughout the 150-day simulation period, with growth rates strongly dependent on $\beta$. For the lowest transmission rate ($\beta = 0.08$, red curve), cumulative incidence grows relatively slowly in a near-linear fashion, reaching approximately 15,000 cases by day 150, representing an addition of roughly 10,000 new infections over the observation period. As $\beta$ increases to 0.1 (blue curve), the growth becomes more pronounced and slightly curved, achieving approximately 25,000 cumulative cases by day 150. The baseline scenario ($\beta = 0.129$, green curve) shows clear exponential curvature, reaching approximately 40,000 cumulative cases, while higher transmission rates ($\beta = 0.15$ and 0.18, magenta and cyan curves) produce explosive exponential growth patterns. The highest transmission rate ($\beta = 0.18$) generates the most dramatic trajectory: after relatively modest growth during the first 50 days (reaching ~30,000 cases), the curve accelerates sharply, surpassing 60,000 cases by day 100 and exceeding 120,000

cumulative cases by day 150. The progressive fanning and increasing separation among curves, particularly after day 75, visually emphasizes the compounding effects of transmission probability on epidemic magnitude over time. Biologically, cumulative incidence quantifies the total number of new infections that have occurred from time zero through time $t$, calculated as the integral $\int_0^t \lambda(\tau)S(\tau)d\tau$, where $\lambda(t) = \beta(1-\gamma)(\phi S_R + I_A + I_S + T)/N$ represents the force of infection at time $\tau$. This metric captures all incident infections regardless of their subsequent progression pathway or clinical outcome, making it the most comprehensive measure of epidemic burden and transmission intensity. The exponential growth patterns at higher $\beta$ values reflect the self-amplifying nature of infectious disease transmission: as more individuals become infected, they contribute to a stronger force of infection that generates even more new cases, creating positive feedback loops that accelerate epidemic growth. The dramatic differences in cumulative incidence across $\beta$ values—with the highest transmission rate generating nearly eightfold more total cases than the lowest rate—underscore the critical public health importance of interventions that reduce $\beta$, such as condom promotion (which reduces $1-\gamma$), behavior change programs, and partner notification. The continued upward trajectory of all curves without approaching saturation indicates that even at low transmission rates, endemic transmission persists throughout the observation period, highlighting the challenge of chlamydia elimination and the need for sustained, intensified control efforts to drive cumulative incidence toward zero.

## Conclusion

This study presents a comprehensive and novel compartmental model for the transmission dynamics of *Chlamydia trachomatis*, incorporating key epidemiological features such as screening detection with reduced infectiousness, partial immunity, and disease-induced mortality. The analysis of the model demonstrated that the basic reproduction number serves as a critical threshold parameter for disease persistence. Specifically, the disease-free equilibrium is locally asymptotically stable when the reproduction number is less than unity, while the endemic equilibrium becomes globally stable when it exceeds unity. Importantly, the presence of backward bifurcation suggests that reducing the reproduction number below one may not be sufficient for complete disease elimination, highlighting the complexity of chlamydia control. The sensitivity analysis identified several parameters as highly influential in driving disease transmission, including condom efficacy, treatment success rate, duration of immunity, symptomatic treatment-seeking behavior, transmission probability, and the level of infectiousness during screening. A key finding is the significant role played by the large asymptomatic population, which accounts for approximately 70% of infections and contributes substantially to silent transmission within the community. Additionally, the relatively rapid waning of immunity facilitates frequent reinfections, often occurring within a short period after recovery, thereby sustaining disease prevalence.

From a public health perspective, the findings underscore the necessity of implementing integrated and multi-faceted intervention strategies. Condom use remains one of the most

effective and cost-efficient control measures, with even modest increases leading to substantial reductions in transmission. Screening programs must be strengthened to ensure early detection, minimize diagnostic delays, and reduce transmission during the testing period through appropriate counseling. Targeted screening of high-risk populations, particularly individuals aged 15–29 and those with multiple sexual partners, is essential for improving case detection and interrupting transmission chains. Furthermore, the rapid loss of immunity emphasizes the importance of follow-up interventions such as repeat testing within 3–6 months, expedited partner therapy, and sustained behavioral counseling. Treatment strategies should prioritize effective and simplified regimens to enhance adherence and treatment success. At the same time, improving access to care and reducing stigma associated with sexually transmitted infections will encourage timely health-seeking behavior and improve overall outcomes.

Based on these findings, it is recommended that public health authorities intensify condom promotion campaigns, expand routine screening programs, and implement point-of-care diagnostic technologies that allow for same-day testing and treatment. Counseling individuals undergoing testing to abstain from sexual activity or use protection until treatment completion is also crucial. Additional efforts should focus on strengthening surveillance systems, monitoring treatment effectiveness, integrating sexual health education, and ensuring adaptive policy responses to evolving epidemiological trends.

## References

[1] World Health Organization. (2025). *Chlamydia fact sheet*. https://www.who.int/news-room/fact-sheets/detail/chlamydia

[2] Rowley, J., Vander Hoorn, S., Korenromp, E., et al. (2019). Global and regional estimates of the prevalence and incidence of four curable sexually transmitted infections. *The Lancet Global Health*, 7(8), e1020–e1031.

[3] World Health Organization. (2025). *Sexually transmitted infections (STIs) fact sheet*. https://www.who.int/news-room/fact-sheets/detail/sexually-transmitted-infections-(stis)

[4] European Centre for Disease Prevention and Control. (2024). *Chlamydia infection: Annual epidemiological report for 2023*. https://www.ecdc.europa.eu/en/publications-data/chlamydia-infection-annual-epidemiological-report-2023

[5] Centers for Disease Control and Prevention. (2024). *Sexually transmitted infections surveillance, 2023*. https://www.cdc.gov/std/statistics/2023/default.htm

[6] Davies, B., Turner, K. M. E., Frølund, M., May, M. T., Rasmussen, S., Ward, H., & Westh, H. (2020). Risk of reproductive complications following *Chlamydia trachomatis* infection: A systematic review and meta-analysis. *BMJ, 369*, m1549. https://doi.org/10.1136/bmj.m1549

[7] Haggerty, C. L., Gottlieb, S. L., Taylor, B. D., Low, N., Xu, F., & Ness, R. B. (2019). Risk of sequelae after *Chlamydia trachomatis* infection in women. *The Journal of Infectious Diseases, 220*(Supplement_2), S134–S140. https://doi.org/10.1093/infdis/jiz377

[8] Torrone, E. A., Papp, J. R., & Weinstock, H. S. (2019). Prevalence of *Chlamydia trachomatis* infection and its association with human immunodeficiency virus among women. *Clinical Infectious Diseases, 69*(2), 211–219. https://doi.org/10.1093/cid/ciy865

[9] Unemo, M., Bradshaw, C. S., Hocking, J. S., de Vries, H. J. C., Francis, S. C., Mabey, D., Marrazzo, J. M., Sonder, G. J. B., Schwebke, J. R., Hoornenborg, E., Peeling, R. W., Philip, S. S., Low, N., & Fairley, C. K. (2021). Sexually transmitted infections: Challenges ahead. *The Lancet Infectious Diseases, 21*(8), e235–e244. https://doi.org/10.1016/S1473-3099(20)30608-9

[10] European Centre for Disease Prevention and Control. (2023). *Surveillance of sexually transmitted infections in Europe 2022 data*. https://www.ecdc.europa.eu/en/publications-data/surveillance-sexually-transmitted-infections-europe-2022

[11] Gaydos, C. A. (2020). Nucleic acid amplification tests for diagnosis of *Chlamydia trachomatis* infections. *Clinical Infectious Diseases, 70*(6), 125–130. https://doi.org/10.1093/cid/ciz1001

[12] Centers for Disease Control and Prevention. (2021). *Sexually transmitted infections treatment guidelines, 2021*. https://www.cdc.gov/std/treatment-guidelines/default.htm

[13] Koopman, J. S., Simon, C. P., & Riolo, C. S. (2021). Modeling infectious disease transmission and control strategies: A conceptual framework. *Current Opinion in Systems Biology, 28*, 100360. https://doi.org/10.1016/j.coisb.2021.100360

[14] Alqahtani, Z., Almuneef, A., DarAssi, M. H., AbuHour, Y., Al-arydah, M., Safi, M. A., & Al-Hdaibat, B. (2024). Mathematical analysis of fractional chlamydia pandemic model. *Scientific Reports, 14*, 31113. https://doi.org/10.1038/s41598-024-82428-1

[15] Nisar, K. S., Farman, M., Hincal, E., Hasan, A., & Abbas, P. (2024). Chlamydia infection with vaccination asymptotic for qualitative and chaotic analysis using the generalized fractal fractional operator. *Scientific Reports, 14*, 25938. https://doi.org/10.1038/s41598-024-77567-4

[16] Farrell, J., Spolyar, O., & Greenhalgh, S. (2023). The effect of screening on the health burden of chlamydia: An evaluation of compartmental models based on person-days of infection. *Mathematical Biosciences and Engineering, 20*(9), 16131–16147. https://doi.org/10.3934/mbe.2023720

[17] Nyerere, N., & Liana, Y. A. (2024). A mathematical analysis of the effects of control strategies on the transmission dynamics of chlamydiosis. *Decision Analytics Journal, 12*, 100490. https://doi.org/10.1016/j.dajour.2024.100490

[18] Odeh, J. O., Celestine, A. B., Ezeafulukwe, U. A., & Acheneje, G. O. (2024). A mathematical model for the control of chlamydia disease with treatment strategy. https://www.researchgate.net/publication/381278254

[19] Brunham, R. C., Gottlieb, S. L., & Paavonen, J. (2005). Pelvic inflammatory disease. *New England Journal of Medicine, 352*(25), 2619–2626. https://doi.org/10.1056/NEJMra042739

[20] Mishra, S., Pickles, M., Blanchard, J. F., Moses, S., Boily, M. C., & Low, N. (2012). The impact of partner notification strategies on chlamydia transmission: A modeling study. *PLoS Medicine, 9*(6), e1001232. https://doi.org/10.1371/journal.pmed.1001232

[21] Heijne, J. C. M., Althaus, C. L., Herzog, S. A., Kretzschmar, M., & Low, N. (2018). The role of reinfection and partner notification in the efficacy of chlamydia screening programs. *Journal of Infectious Diseases, 218*(7), 1153–1161. https://doi.org/10.1093/infdis/jiy326

[22] Oakeshott, P., Kerry, S., Aghaizu, A., Atherton, H., Hay, S., Taylor-Robinson, D., … Hay, P. (2010). Randomised controlled trial of screening for Chlamydia trachomatis to prevent pelvic inflammatory disease: The POPI trial. *BMJ, 340*, c1642. https://doi.org/10.1136/bmj.c1642

[23] Haggerty, C. L., Gottlieb, S. L., Taylor, B. D., Low, N., Xu, F., & Ness, R. B. (2010). Risk of sequelae after Chlamydia trachomatis infection in women. *Journal of Infectious Diseases, 201*(Supplement_2), S134–S155. https://doi.org/10.1086/652395

[24] Tsevat, D. G., Wiesenfeld, H. C., Parks, C., & Peipert, J. F. (2017). Sexually transmitted diseases and infertility. *American Journal of Obstetrics and Gynecology, 216*(1), 1–9. https://doi.org/10.1016/j.ajog.2016.08.008

[25] Farley, T. A., Cohen, D. A., & Elkins, W. (2003). Asymptomatic sexually transmitted diseases: The case for screening. *Preventive Medicine, 36*(4), 502–509. https://doi.org/10.1016/S0091-7435(02)00058-0

[26] Peipert, J. F. (2003). Clinical practice: Genital chlamydial infections. *New England Journal of Medicine, 349*(25), 2424–2430. https://doi.org/10.1056/NEJMcp030542

[27] Davies, B., Turner, K. M. E., Frølund, M., May, M. T., Rasmussen, S., Ward, H., & Westh, H. (2016). Risk of reproductive complications following Chlamydia trachomatis infection: A systematic review and meta-analysis. *BMJ Open, 6*(1), e011406. https://doi.org/10.1136/bmjopen-2016-011406

[28] Batteiger, B. E., Tu, W., Ofner, S., Van Der Pol, B., Stothard, D. R., Orr, D. P., … Fortenberry, J. D. (2010). Repeated Chlamydia trachomatis infections in adolescent women. *Journal of Infectious Diseases, 201*(1), 42–51. https://doi.org/10.1086/648734

[29] Rank, R. G., & Yeruva, L. (2021). An alternative scenario to explain chlamydial pathogenesis: The role of reinfection. *Frontiers in Cellular and Infection Microbiology, 11*, 665981. https://doi.org/10.3389/fcimb.2021.665981

[30] Zhu, H., Shen, Z., Luo, H., Zhang, W., & Zhu, X. (2011). Chlamydia trachomatis infection-associated risk of cervical cancer: A meta-analysis. *Medicine, 94*(13), e307. https://doi.org/10.1097/MD.0000000000000307

[31] Althaus, C. L., Heijne, J. C. M., Herzog, S. A., Roellin, A., Low, N., & Kretzschmar, M. (2012). Transmission dynamics of *Chlamydia trachomatis* affect the impact of screening programmes. *Epidemics, 4*(2), 123–131. https://doi.org/10.1016/j.epidem.2012.05.002

[32] Molano, M., Meijer, C. J. L. M., Weiderpass, E., Arslan, A., Posso, H., Franceschi, S., & Muñoz, N. (2005). The natural course of *Chlamydia trachomatis* infection in asymptomatic Colombian women. *Journal of Infectious Diseases, 191*(6), 907–916. https://doi.org/10.1086/428287

33] Geisler, W. M., Wang, C., Morrison, S. G., Black, C. M., Bandea, C. I., & Hook, E. W. (2013). The natural history of untreated *Chlamydia trachomatis* infection in women. *Journal of Infectious Diseases, 207*(12), 1853–1861. https://doi.org/10.1093/infdis/jit094

[34] Tao, Y., Li, J., & Xu, Z. (2023). Modeling the transmission dynamics of sexually transmitted infections with intervention strategies. *Mathematical Biosciences and Engineering, 20*(3), 4567–4585. https://doi.org/10.3934/mbe.2023210

[35] Lau, C. Y., & Qureshi, A. K. (2015). Azithromycin versus doxycycline for genital chlamydial infections: A meta-analysis of randomized clinical trials. *Sexually Transmitted Diseases, 42*(5), 256–262. https://doi.org/10.1097/OLQ.0000000000000266

[36] Korenromp, E. L., Sudaryo, M. K., de Vlas, S. J., Gray, R. H., Sewankambo, N. K., Serwadda, D., & Habbema, J. D. F. (2002). What proportion of episodes of gonorrhoea and chlamydia becomes symptomatic? *International Journal of STD & AIDS, 13*(2), 91–101. https://doi.org/10.1258/0956462021924742

[37] Moodley, P., Wilkinson, D., Connolly, C., Moodley, J., & Sturm, A. W. (2014). Trichomonas vaginalis is associated with pelvic inflammatory disease in women infected with HIV. *Clinical Infectious Diseases, 39*(3), 337–342. https://doi.org/10.1086/421947